Australian Government

Wine Australia

Smartphone based image analysis to assess vine water stress

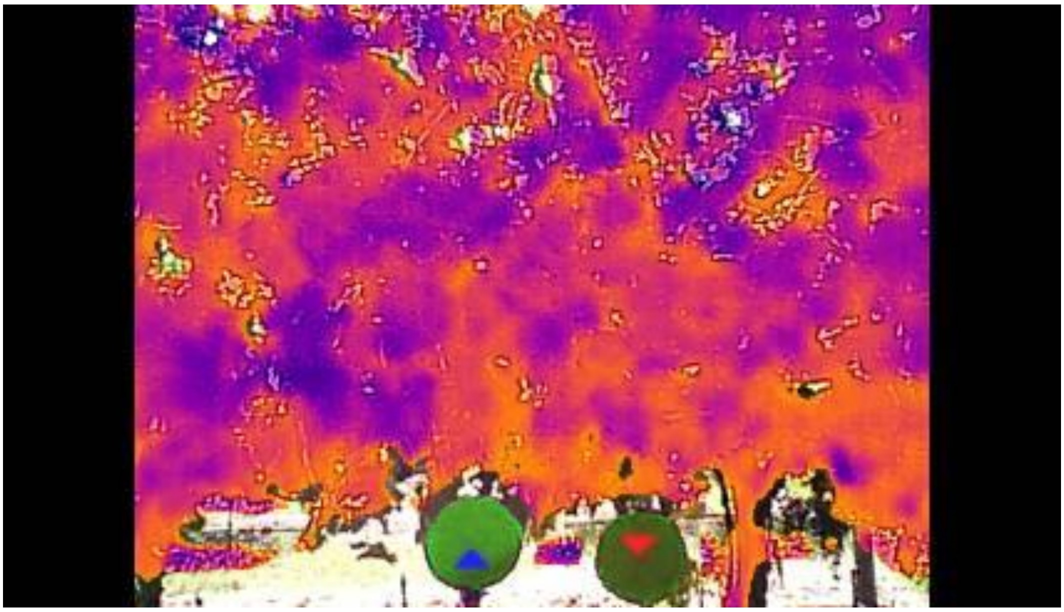

FINAL REPORT to

WINE AUSTRALIA

Project Number: **SAR 1501**

Principal Investigator: **Mark Skewes**

Research Organisation: **South Australian Research and Development Institute**

Date: **6 February 2018**

South Australian Research and Development Institute

SARDI Sustainable Systems

Waite Research Precinct

Plant Research Centre

2b Hartley Grove

Urrbrae SA 5064

email: mark.skewes@sa.gov.au

Table of Contents

Abstract

Smartphones have advantages over specialist systems for extending crop monitoring, including ubiquity, price, user familiarity and ease of implementing updates.
This project evaluated a range of smartphone based tools for measuring vine water status. Irrigation deficit treatments were applied to grapevines in the Riverland of South Australia. Water status measurements from smartphone based sensors were benchmarked against conventional methods including stem water potential and stomatal conductance.
A thermal infrared camera system was selected as the most accurate and robust option for development into an app, which was tested by viticulturists in 2017.

Executive summary

Smartphones contain a variety of sensors that have the potential to monitor the surrounding environment and provide an aid to decision making across a range of industries, from medicine through to agriculture. Smartphones have several advantages over specialist monitoring systems, including ubiquity, price, user familiarity and the ease of implementing updates. They also contain sufficient computing power, so the analysis and support software can be contained within the phone.

A range of methods has been developed for the assessment of vine water status – however none currently meets the affordability, portability and ease of use requirements for wide scale adoption. A wide range of sensors could potentially be interfaced with smartphones to assess vine moisture status. The aim of this project work was to evaluate a range of smartphone based tools for measuring vine water status, leading to the development of the most promising tool into a smartphone application that can be easily used by vineyard managers.

Systems that were evaluated included:

- An infrared camera that is integrated into or connected directly to the smartphone and uses established techniques for the analysis of thermal imagery to assess water status;
- A portable Near Infrared spectrophotometer that interfaces with the phone and measures reflectance across relevant wavelengths for the calculation of water status indices;
- A 3D camera that is integrated into or connected to the phone via Wi-Fi and can use image analysis to assess the shape or orientation of the leaves;
- A microscope attached to the smartphone camera or as a separate portable unit that can be used to measure stomatal number and aperture and then calculate stomatal conductance.

A trial site with a range of irrigation deficit treatments applied to Chardonnay and Cabernet Sauvignon grapevines was established in the Riverland of South Australia. Water status measurements from the smartphone based sensors described above were benchmarked against conventional methods including mid-day stem water potential and stomatal conductance.

The thermal infrared camera system, measuring the Crop Water Stress Index (CWSI), was selected as the most accurate and robust option for development into an app. The app was tested during the 2017 growing season to demonstrate its accuracy and confirm that the most appropriate indices were being used. User acceptance testing was also completed by viticulturists to assess its utility with further improvements being made during the season based on feedback from this testing. Positive feedback on the utility of the app was received from the beta testing group. Over the 33 days of formal assessment, the CWSI, as calculated by the app, had a strong relationship with the reference methods of mid-day stem water potential ($R^2 = 0.62$) and stomatal conductance ($R^2 = 0.74$).

There is a range of scenarios where CWSI could be used to inform irrigation scheduling, which could complement or replace existing soil moisture monitoring systems. Regular assessment of the CWSI in a vineyard will help develop an understanding of what values to expect from different blocks or varieties. If the target is to maximise vineyard yield then water stress needs to be avoided, while not applying excessive water. Checking the CWSI immediately prior to applying irrigation would confirm that no stress had occurred. Preliminary estimates suggest that a CWSI of less than 0.7 recorded from a shaded canopy on a hot day, or 0.5 on a cooler day would indicate vines are well irrigated. If the target is to optimise quality and minimise water use as part of a regulated deficit irrigation strategy, then the CWSI could also be used to inform irrigation decisions. If the vines are being maintained at a moderate water deficit (for example during the post flowering period) then irrigation could be withheld if the CWSI is below approximately 0.8 assuming very hot weather is not forecast. Tracking the CWSI over time may give a viticulturist more confidence to extend the period between irrigation applications. Soil moisture monitoring systems are normally point based at a limited number of sites across a vineyard; it is uncommon for all the blocks within a vineyard to be covered. The thermal camera is very portable and can be used to compare different parts of a block and across blocks. This system provides an easy opportunity to check sections of a block that may not be receiving enough water, and benchmark these against the section adjacent to the soil moisture probe.

If the app is developed further and maintained so that it can be used by the wine industry, then the savings in water applications are likely to occur as growers will be able to easily assess their vineyards irrigation needs. Fruit quality will also potentially be improved through the better management of regulated water deficit, and by applying strategic irrigations to maintain canopy health and avoid defoliation.

This project was completed as a collaboration between the South Australian Research and Development Institute (SARDI) and the University of New South Wales (UNSW). The measurement of vine water status was completed by SARDI at the Loxton Research Centre, and the image analysis and app development were completed by UNSW in Sydney.

Background

Smartphones contain or can be attached to a variety of sensors that have the potential to monitor the surrounding environment and provide an aid to decision making across a range of industries, from medicine through to agriculture. Smartphones have many advantages over specialist monitoring systems including ubiquity, price, user familiarity and the ease of implementing updates; they also contain sufficient computing power, so that the analysis and support software can be contained within the phone (Ozdalga et al. 2012).

A range of methods has been developed for the assessment of vine water status – however none currently meet the portability and ease of use requirements for wide scale adoption. Measures of water availability in the agricultural environment are important both for the efficient use of a valuable and increasingly scarce resource (e.g. Gerten et al. (2011)) and to produce high quality produce (Fereres and Evans 2006). There is a wide range of plant and soil water status assessment systems available for commercial use in Australia (Charlesworth 2005, White and Raine 2008), with soil based sensors being by far the most popular in Australian viticulture where use is reported by more than 60% of growers (Green and Griffante 2009). Soil based systems are often preferred in the commercial environment because of their robustness, few maintenance requirements, familiarity among users and suppliers and low skilled labour requirements once installed (Charlesworth 2005).

An easy, portable and cost-effective system for the direct and real-time assessment of vine water status remains a challenge for all agricultural industries (Jones 2004). As water resources become scarcer, the use of irrigation to optimise yield and quality will only increase in importance to the industry. Plant based monitoring systems are often used in a research context, but unfortunately their application to commercial production has been limited (Naor 2006). The direct indication of plant water status and ability to avoid symptoms that result in a reduction in productivity or quality are key positive attributes of measuring plant water status (Jones 2004). In addition, most soil based sensing systems, especially those designed to measure to a depth (1m and below) relevant for perennial crops, are point based and do not allow variation across an orchard or vineyard to be easily assessed. Plant based sensors are often far more portable as they can be easily moved between plants.

Water potential (pre-dawn, leaf and stem) as measured by the Scholander pressure chamber (Scholander et al. 1964) is the most widely accepted direct sensing method (Jones 2004). There are several limitations to the commercial use of this technique in Australian viticulture, including the extensive labour requirements, operator safety, inconsistency between operators and the requirement for leaf pre-bagging.

Alternative measurement techniques including infrared cameras and leaf NIR spectrometry have been researched; however, we are not aware of any commercial systems that are available in these areas. The cost of hardware and specialist systems is a likely impediment to their development. Smartphones are a ubiquitous business tool and are the ideal mount for a plant based water sensor, given their portability and ease of access to software updates. They are generally equipped with high resolution cameras, or can have specialist sensors such as microscopes, stereo cameras, thermal cameras or spectrometers attached.

The development of a smartphone based system to assess water stress in vines would promote the broader uptake of water stress monitoring across the viticulture industry, potentially improving water use efficiency and fruit quality. We investigated four smartphone based systems, to determine their viability to assess vine water status.

Spectroscopy

Near infrared (NIR) spectroscopy is a commonly used, non-destructive method to analyse components of agricultural and food products (e.g. Cozzolino et al. (2006)). The NIR region of the electromagnetic spectrum (730–2300 nm) contains wavelength ranges that are affected by the sample water content or concentration. These include strong NIR absorption bands of water around 1400–1440 nm and between 1900 to 1950 nm, which have often been applied to the quantitative analysis of water content in food (e.g. Cozzolino et al. (2006)). Wavelength bands related to water have also been utilised in NIR reflectance with proximal and remote sensing applications to determine water content and water status of plants (e.g. Peñuelas et al. (1993)). De Bei et al. (2011) evaluated the measurement of the water status of grapevines using a spectrophotometer; compared to midday leaf water potential measured on an adjacent leaf on the same shoot. The NIR showed good predictive ability for stem water ($\Psi_{stem)}$ potential for each of the three grapevine varieties assessed, suggesting that NIR can be used as a simple and rapid method to detect grapevine water status. Unfortunately, the equipment used to complete this analysis was very expensive (more than $25,000), meaning that it is not easily accessed by growers.

Camera based leaf angle

The canopy morphology (leaf orientation and angle) changes as water stress develops in grapevines (and most other plants). Experienced managers can tell if irrigation is required based on observation – however this is largely intuitive with no direct relationship between canopy appearance and water stress. Research in the 1970s demonstrated a relationship between the angle formed between the leaf midrib and the petiole with vine water stress (Smart 1974); however, collecting these measurements was very onerous. Stereo vision makes use of the disparity between two offset cameras to build a depth map which represents the scene in three dimensions as viewed from the perspective of the camera. More recently a stereo camera and a local edge detection algorithm were used to make simple measurements of leaf angles (relative to the ground) and these were used as an indication of water stress (Mizuno et al. 2007). Image analysis of photos collected by a smartphone may be able to determine these leaf traits in real time based on the angle or the cupping of the leaves.

Stomatal aperture

The stomata are the pores on the leaf that regulate the gas flow (stomatal conductance, g_S) and control photosynthesis and transpiration. Under water stress conditions the stomata will close to prevent the leaves desiccating. The stomata are small and cannot be seen with the naked eye. Currently, stomatal number and aperture are assessed by taking an imprint of the leaf and analysing this under a microscope in the lab, however these measurements aren’t used for irrigation scheduling Sadras et al. (2012). Stomatal number and aperture have also been assessed directly (usually in the lab) using a camera mounted in an optical microscope (Kappen et al. 1995). There is a variety of high powered magnifying attachments (up to 200x) available for smartphone cameras that may allow images of suitable quality to be collected so that stomatal aperture, and the proportion of closed stomata can be assessed in the field. If the area of the open stomata pores, relative to the image (or leaf) area is known then the g_S can be calculated (Lawson et al. 1998), if this method is to be used successfully then a sampling regime to overcome the impact of stomatal patchiness would also be needed (Düring and Stoll 1996).

Thermal imaging

An alternative plant based method of assessing water status is based on the measurement of water use by the plant. This is assessed as g_S to water vapour or the transpiration (similar to evaporation) of water from the leaf/canopy. This can be completed by using a porometer or other devices that can directly measure the gas exchange of individual leaves; however, the logistics of measuring individual leaves across a canopy make these methods difficult (Costa et al. 2013). As a surrogate for the direct measurement of water loss by leaves, leaf (or canopy) temperature can be measured, based on the principle that the reduction in temperature is proportional to the amount of water lost from the leaves and the associated evaporative cooling. On this basis when the stomata close, transpiration stops, and the leaf temperature increases; when the stomata open, transpiration increases and canopy temperature drops (Brown and Escombe 1905).

The principle that infrared thermometry can be used as an indicator of plant water stress was first developed in the 1960s (Tanner 1963), and the technological improvements over the last 50 or more years has allowed the refinement of these techniques for the assessment of plant water status. Infrared cameras are now available that are integrated into or able to be connected directly to the smartphone. These systems can potentially be used to assess the irrigation requirements of crops and meet the portability and ease of use requirements for wide scale adoption. Solutions have been developed that allow g_S to be estimated directly from canopy temperature and a range of other meteorological inputs (Guilioni et al. 2008, Leinonen et al. 2006). In addition, simple indices have been developed that can convert the canopy temperature measurements into a value suitable for irrigation scheduling, such as the Crop Water Stress Index (CWSI).

Project Aims and Performance targets

This project aimed to evaluate a range of smartphone based sensing systems and to develop a system that can assess vine water stress in an accurate and reproducible manner. This method would be developed into a smartphone application and user acceptance testing completed to integrate the preferred technology into a tool to assess vine water status.

The project was split over two seasons; the first season focused on assessing the hardware and software options for each of the four proposed techniques:

- Spectrometer (SCiO molecular sensor)
- 3D Camera based leaf angle (Stereo camera system; GoPro and Fujifilm FinePix Real 3D)
- Stomatal aperture (Smartphone based microscopes, ProScope Micro Mobile, ProScope EDU and ProScope HR2)
- Thermal Camera (FLIR One and Seek).

At the end of the first season the accuracy of each of the techniques was assessed, and the preferred candidate technology selected based on accuracy and ease of use. Measurements were conducted at the SARDI Loxton Research Centre and image analysis was completed at the UNSW in Sydney. Development of the beta version of the app was completed by a contractor working with the UNSW.

The preferred assessment system (the FLIR One, thermal camera) was chosen on the completion of the first season of assessments. During the second season the technique was validated based on measurements taken from vines at the Loxton Research Centre. The image analysis process and calibration of the results against standard methods were refined by UNSW. Beta testing of the application was completed by potential users across a range of regions and varieties and feedback on the app utility and how it could be improved was sought. The app was improved during the season based on feedback from the beta testers.

Method

Four methods of estimating vine water status, that could potentially be based on a smartphone, were compared to stem water potential (Ψ_{stem}, measured with a pressure chamber), and stomatal conductance (g_S, measured using a porometer).

Trial site and sampling regime

Trial vines were located at the Loxton Research Centre, and consisted of a plot of Cabernet Sauvignon managed to four irrigation levels (namely 100%, 75%, 50% and 12.5% of evapotranspiration throughout the season), and a plot of Chardonnay both fully irrigated (100% evapotranspiration) and a deficit irrigation regime imposed two weeks prior to the first assessments of vine water status. Measurements of vine water status were collected on the six treatments (four Cabernet Sauvignon and two Chardonnay) on five dates during February and March 2016 (season one) and 33 dates between December 2016 and March 2017 (season two). On every date, reference measures including g_S (porometer) readings from four shaded leaves and Ψ_{stem} (pressure chamber) from three leaves per vine were collected (see below). During season one, vines were assessed using the four potential analysis methods, spectrometer, 3D Camera based leaf angle assessment, imaging of stomatal aperture and thermal imaging of canopy temperature (more details on these methods are provided below). The aim of sampling across a range of dates was to provide a wide range of weather conditions so the robustness of all techniques could be assessed.

Reference methods

Two standard measures of vine water status were used. Measurements of Ψ_{stem} were made using a pressure chamber; model 3000 (Soil Moisture Equipment Corporation, Santa Barbara, CA, USA) with the standard analog gauge replaced with a 0-5 MPa digital gauge (DG 25, Ashcroft, Stratford, Connecticut, USA). The method of Choné et al. (2001) was followed; briefly, leaves were enclosed in an aluminium foil covered bag for at least one hour prior to measurement so that leaf water potential could equilibrate with Ψ_{stem}. Measurements of g_S were made using a SC-1 Leaf Porometer (Decagon Devices, Pullman, Washington, USA), following the operating instructions for this device.

Spectroscopy

The SCiO^{TM} Pocket Spectrometer (Consumer Physics, Tel-Aviv, Israel) uses the Bluetooth protocol to communicate with a smartphone, which acts as a controller and provides access to the internet for cloud based data analysis. The SCiO^{TM} was used to capture reflectance responses across a narrow band of wavelengths (740 to 1070 nm) from ten leaves on each treatment vine on each data collection date during season one. A white tile was used as a backing for the leaf, as results varied when different backing materials were used. The resulting spectral signatures were analysed against Ψ_{stem} and g_S using the proprietary multivariate statistical software on the SCiO^{TM} Lab website (https://sciolab.consumerphysics.com/). For this analysis, wavelengths in the 870-1000 nm range were used and the spectra were pre-processed by subtracting the minimum values and then taking the second derivative prior to calculation of the partial least squares regression. The Water Band Index was also calculated based on the reflectance at 970 nm divided by the reflectance at 900 nm (Peñuelas et al. 1993) and this was compared to the results from the reference methods.

Stomatal aperture

Three microscopes that could be attached to a smartphone were trialled, the ProScope Micro Mobile (80x magnification), ProScope EDU (300x magnification), and ProScope HR2 (400x magnification). The microscope systems were all manufactured by Bodelin Technologies Wilsonville, OR, USA. The Micro Mobile was able to use the smartphone camera, while the other systems used their own cameras as well as lighting and optics. There are many similar products on the market, unfortunately most have exaggerated magnification and resolution claims that include the size that the image will appear on a computer monitor. There was a delay in the delivery of the highest resolution microscope, so as a substitute, nail polish stomatal peels (Gitz and Baker 2009, Meister and Nordenkampf 2001) were collected from leaves so the image analysis and sampling regime could be further developed if this approach appeared promising. The images of the stomatal peels were analysed using a cascade object detection algorithm; in this case the Viola-Jones face detection algorithm was retrained to detect stomata (Viola and Jones 2004). Cascade object detection is well suited to this analysis as it assumes that a large proportion of the image does not contain the object of interest and the aspect ratio does not change significantly. Once the Regions of Interest (ROIs) containing the individual stomates had been identified, the ROIs were binarised and skeletonised to detect the actual pore. More detail on the analysis method is presented in Jayakody et al. (2017), please refer to the Communications section.

3D Camera based leaf angle

The three-dimensional images were taken with two GoPro Hero3+TM cameras mounted in the 3D Dual Hero System (both GoPro, San Mateo, California, USA) and linked to a smartphone to provide a viewfinder capability. Images were also collected using a FinePix Real 3D camera (Fujifilm, Minato, Japan). The leaves were displayed with a black cardboard backing with a hole to allow the petiole through. The black backing ensured the leaves were easily distinguishable from the background and a scale was included to allow the leaf size and shape to be calculated. Two methods were trialed in order to measure leaf shape or cupping.

1) The scale-invariant feature transform (SIFT) algorithm was used to identify and match the location of features (nominally the leaf edges) between the two leaf images. This technique relies on identifying the same location on each of the paired images to calculate their locations in three dimensions.
2) A Structure from Motion (SfM) technique (Zhang et al. 2016) was used to develop a 3D point cloud from the pair of stereo images. The point cloud was then examined to determine the degree of cupping.

Thermal imaging – Season 1

Two smartphone based thermal camera systems, the FLIR™ One (Wilsonville, Oregon, USA) and the Seek™ Thermal (Santa Barbara, California, USA) were benchmarked against a professional thermal camera (FLIR B365, FLIR Wilsonville, Oregon, USA) during the first season. The Seek™ Thermal had a 206 x 156 pixel resolution sensor, a 36° diagonal field of view and a manual focus lens. The long wave infrared sensor had a range of 7.5 to 14 μm and the camera could measure over a temperature range of -40°C to 330°C. The Seek™ application allowed the user to move between an image from the smartphone camera and the thermal image to make orientation easier (Anon 2015a). The FLIR™ One (Wilsonville, Oregon, USA) thermal camera was selected for this project, it has a 160 x 120 pixel resolution. The system includes a second VGA (640 x 480 pixel resolution) camera mounted

adjacent to the thermal sensor, and software that generates an overlay which defines the border of the objects in the image making it easier to orientate and focus. The camera has a long wave infrared sensor with a range from 8 to 14 µm and the lens has a field of view of 46^o horizontal and 35^o vertical. The camera measured over a temperature range of -20^{o}C to 120^{o}C (Anon 2015b).
The crop water stress index (CWSI) was calculated based on the equation modified from Idso (1982) by Jones (1999) for the use of wet and dry reference leaves:

$$CWSI = \frac{T_{canopy} - T_{wet}}{T_{dry} - T_{wet}}$$

Where T_{canopy} is the shaded canopy temperature (^{o}C) obtained from the thermal image, and T_{dry} and T_{wet} are the reference temperatures (^{o}C). T_{dry} was initially obtained by painting the abaxial side of the leaf with petroleum jelly ($T_{dry(pet)}$) (Vaseline, Unilever, London, U.K.) (Idso 1982, Jones 1999). T_{wet} was the temperature of leaves regularly sprayed with water and a little dishwashing soap during measurements ($T_{wet(leaf)}$).
Images were collected from the shaded side of the canopy for all measurements, as this allowed the assessment of vine water status across a wider range of conditions, especially intermittent cloud cover. The canopy temperature and the wet and dry reference temperatures were manually selected using the rectangular or circular selection tools respectively, and extracted from the images using the FLIR Tools™ software.

Thermal imaging – Season 2

During the second season the application development and further validation of the methods focused on using the FLIR™ One thermal camera. Applying water or petroleum jelly directly to leaves was unlikely to be a practical option for growers, so a range of fabric references was tested as alternatives to real leaves. This also allowed the reference surfaces to be coloured, which made them easier to identify in the images. T_{dry} was replicated using a red fabric reference surface ($T_{dry(fab)}$) similar to Maes et al. (2016), but coloured red, a detached leaf ($T_{dry(leaf)}$) was also trialled. T_{wet} was also replicated using a fabric reference surface ($T_{wet(fab)}$) again similar to Maes et al. (2016), and coloured red. A fabric wick was submerged in a bottle of water to ensure that the $T_{wet(fab)}$ remained moist. A range of terrycloth fabrics was evaluated for the $T_{dry(fab)}$ and $T_{wet(fab)}$ during initial testing and significant differences in the relationship between fabric and leaf based reference surfaces were observed. To have a consistent supply of fabric that could be easily accessed by growers or researchers we selected a towel that was distributed globally (Fräjen, IKEA, Leiden, Netherlands).
Other temperature based indices of crop water status are available, and these were also assessed during the second season. These indices are potentially more accurate under humid conditions or would allow water stress to be assessed without the need for the T_{dry} or T_{wet}.

The CWSI can be rearranged as proposed by Jones (1999) to give the conductance index (Ig):

$$Ig = \frac{T_{dry} - T_{canopy}}{T_{canopy} - T_{wet}}$$

Where Ig is proportional to the g_S and therefore decreases as the stomata close and the differential between the T_{wet} and the T_{canopy} increase. The Ig is more sensitive to changes in plant water status when the water deficit is low, making it suitable for use in humid conditions or where less water stress is present (Jones 1999).

A series of formulae has also been derived from the basic leaf energy balance (Jones et al. 2002) to calculate g_S directly from canopy temperature and a combination of environmental variables and reference leaf temperatures (Guilioni et al. 2008, Leinonen et al. 2006). These formulae potentially offer the advantage of allowing plant water status to be calculated based on meteorological parameters (collected by a weather station adjacent to site) without the requirement to erect the wet and/or dry reference surfaces.

The first formula is calculated directly based on canopy temperature and environmental parameters (net isothermal radiation, wind speed, air temperature and relative humidity), (Leinonen et al. 2006):

$$g_{s(no\ ref)} = \frac{1}{-\rho \times c_p \times r_{HR} \times (s(T_{canopy}-T_{air})+D)/(\Upsilon(T_{leaf}-T_{air}) \times \rho \times c_p - r_{HR} \times R_{ni}))-r_{aW}}.$$

Where ρ is the density of air (kg.m^{-3}), c_p is the specific heat capacity of air (J.Kg^{-1}.K^{-1}), s is the slope of the curve relating saturated water vapour pressure to temperature (Pa.^{o}C^{-1}), r_{HR} is the parallel resistance to heat and radiative transfer (s.m^{-1}), D is the air vapour pressure deficit (Pa), Υ is the psychrometric constant (Pa.K^{-1}), R_{ni} is the net isothermal radiation (the net radiation for a leaf at air temperature (W.m^{-1}) and r_{aW} is the leaf boundary layer resistance to water vapour (s.m^{-1}).

The second formula avoids the need for the measurement of absorbed radiation by using T_{dry} (Leinonen et al. 2006):

$$g_{s(dry)} = \frac{1}{-\rho \times c_p \times r_{HR} \times (s(T_{canopy}-T_{air})+D)/(\Upsilon(T_{leaf}-T_{air}) \times \rho \times c_p \times (T_{canopy}-T_{dry})))-r_{aW}}.$$

Complementing the above calculations; g_S can also be calculated based on environmental parameters and the wet and dry reference surfaces. The most appropriate formula for grapevines assumes the reference surface is wet on both sides and the leaves are hypostomatous (stomata on the lower side) (Guilioni et al. 2008).

$$g_{s(dry\&wet)} = \frac{1}{(r_{aW}/2 + (s/\Upsilon) \times r_{HR}) \times (T_{canopy} - T_{wet})/(T_{dry} - T_{canopy}) - r_{aW}/2}.$$

For the automatic detection of the canopy temperature and wet and dry reference temperatures, the images were analysed as follows. The thermal image in the proprietary FLIR^{TM} MSX format was processed using a 7 x 7 pixel gaussian smoothing filter to reduce noise. A binary reference mask corresponding to the red areas in the RGB image (the wet and dry references) was generated by converting the RGB (Red, Green, Blue) image to HSV (Hue, Saturation, Value) format and selecting the red portion of the image as having values, H: 328 – 366, S: 0.47 – 1.0 and V: 0.21 – 1.0. Noise (random variation across the binary image) was removed using two series of filters of different sizes. A 5 x 5 pixel erode filter and then a 7 x 7 pixel dilate filter were used to remove speckles followed by a 11 x 11 pixel erode filter and a 9 x 9 pixel dilate filter to close any gaps. The filter was also applied to the thermal image with a 15-pixel inset to avoid errors due to poor focus of the thermal image or misalignment of the original RGB and thermal images. The thermal data in the wet and dry references were divided into contours at 0.1^{o}C intervals and the warmest (dry reference) and coldest (wet reference) section of the image, that was greater than 50 pixels in size, was selected.

To calculate the canopy temperature a second binary mask was created from the thermal image. All sections of the image that contained temperatures that were hotter than the dry reference and cooler than the wet reference were excluded (Fuentes et al. 2012). The image noise and potential errors due to poor focus were managed using the filters and inset described above. Both filters were applied to the RGB image, so it could be displayed on the screen of the smartphone to allow the user to check that the filter had worked correctly and highlighted the wet and dry references. Originally a slider bar was provided to allow the upper and lower temperature thresholds to be adjusted to better define the portion of the image that was considered canopy; however, this feature was found difficult to use by the user acceptance testers (see below). The canopy was occasionally not well defined in test images so an additional binary filter, to exclude the background (non-canopy) from the image was added. The filter was based on a Naïve Bayes classifier trained on the RGB images of the canopy. This is a supervised classification technique for constructing classifiers of a probabilistic graphical model. The canopy temperature was automatically calculated from the remaining portion of the image once the masks were used to exclude the image background and the reference surfaces. Once again, a 15-pixel inset was used to avoid errors due to poor focus of the thermal image or misalignment of the original RGB and thermal images.

User acceptance testing

For user acceptance testing a system was distributed to 16 reviewers comprising the FLIR™ One and an Android Smartphone (A1601, Oppo, Dongguan, Guangdong, China). The application was configured to automatically synchronise measurements with a server every time the phone was connected to Wi-Fi (a SIM card was not installed), this allowed camera usage to be tracked and diagnostics easily provided for any user issues. The application and its instructions were refined and updated throughout the 2016-17 growing season, with updates to the software version uploaded to the phones when they were connected to Wi-Fi. Refinements included changes in the CWSI formula to account for differences between the $T_{dry(pet)}$ and $T_{dry(fab)}$, and $T_{wet(leaf)}$ and $T_{wet(fab)}$. Improvements to the system for the automatic delineation of the canopy (see above) meant that the slider bar to help exclude the image background based on temperature could be removed. After harvest the user acceptance testers were surveyed around the utility of the application and their intentions for further use if it was made publicly available (Table 1), this was followed up by a phone or in person interview.

Results and discussion

Spectroscopy

The SCiO was able to collect leaf reflectance spectra across the range of wavelengths from 740 to 1070 nm including the range from 870 to 1000 nm which contains the region that is highly sensitive to water (Figure 1 and Figure 2). The app required a connection to the internet via a smartphone for the spectrophotometer to work effectively. Variable mobile phone coverage at the trial site Loxton sometimes limited the operation of the spectrometer, but overall the equipment performed adequately. The SciO software allowed the development of models by which spectrometer measurements were used to estimate measured parameters, in this case Ψ_{stem} and g_S, and then analysed the relationship between the measured and estimated values. The partial least squares (PLS) model generated for the Ψ_{stem} (Figure 3, r^2 0.78) was much more reliable than the model developed for g_S (Figure 4, r2 0.36). The model was less accurate low measured water potential values, with the estimated values remaining relatively high, indicating that the spectrometer was unable to differentiate MDSWP at values below -1.5 MPa. The relationships between Water Balance Index and Ψ_{stem} or g_S was very poor, and this is unlikely to be a useful metric when collected using the SCiO (Figure 5 and Figure 6).

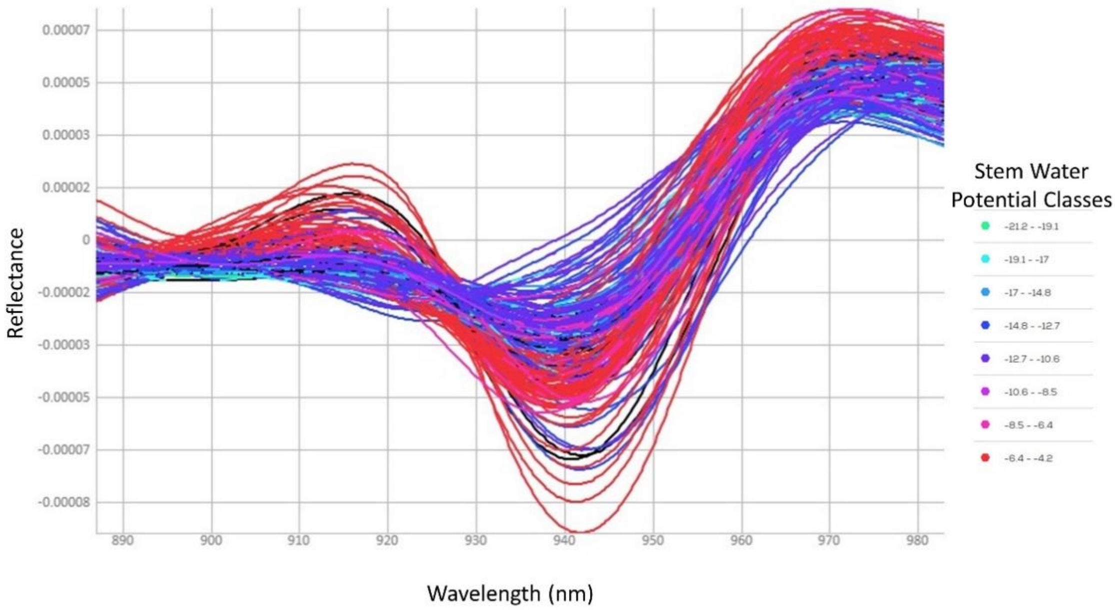

Figure 1
Reflectance spectra of Cabernet Sauvignon leaves collected by the SCiO and grouped by Ψ_{stem}. Spectra have been processed by subtracting the minimum values and calculating the second order derivative.

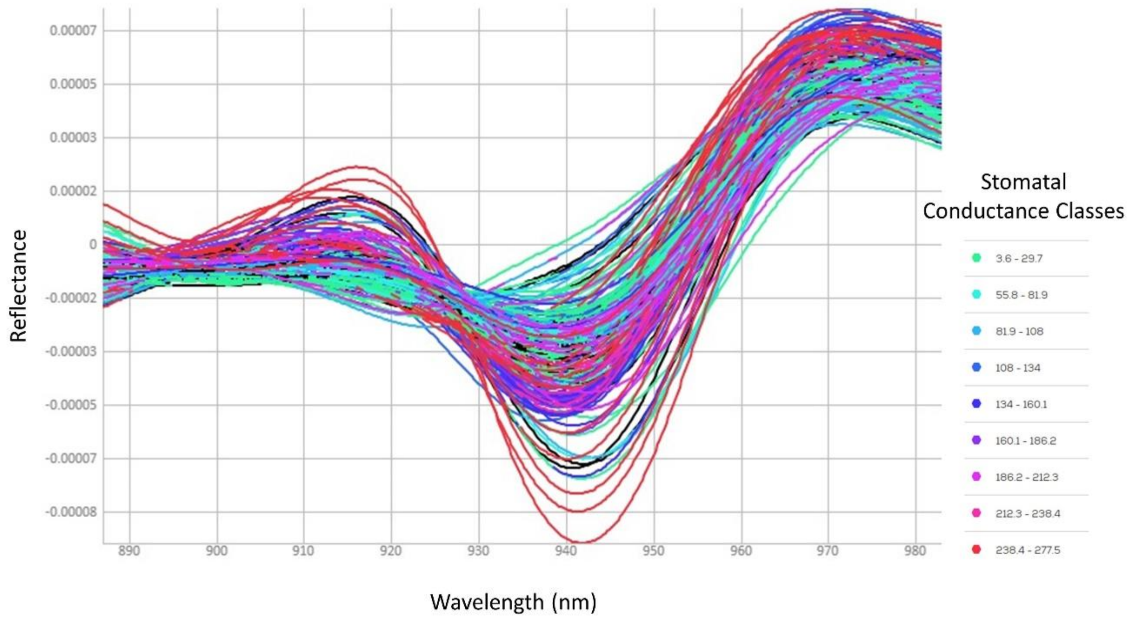

Figure 2
Reflectance spectra of Cabernet Sauvignon leaves collected by the SCiO and grouped by g_S. Spectra have been processed by subtracting the minimum values and calculating the second order derivative.

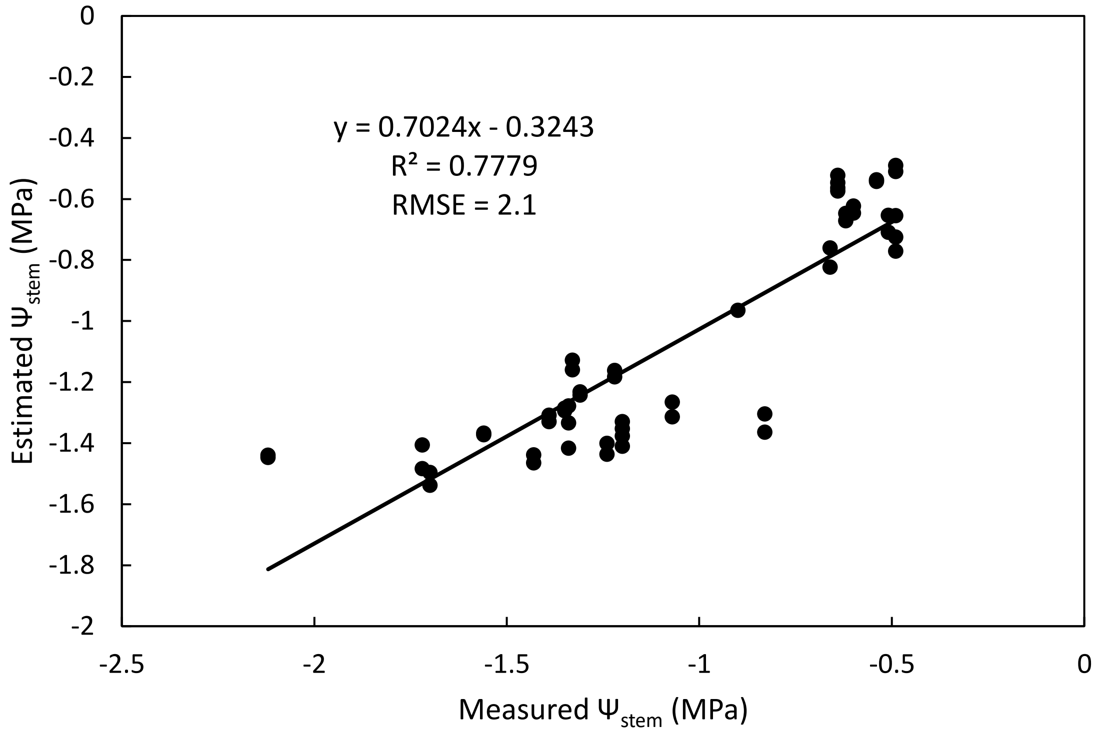

Figure 3
Relationship between the Ψ_{stem} measured using a pressure chamber and the estimated Ψ_{stem} based on leaf spectral reflectance collected by the SCiO for Cabernet Sauvignon.

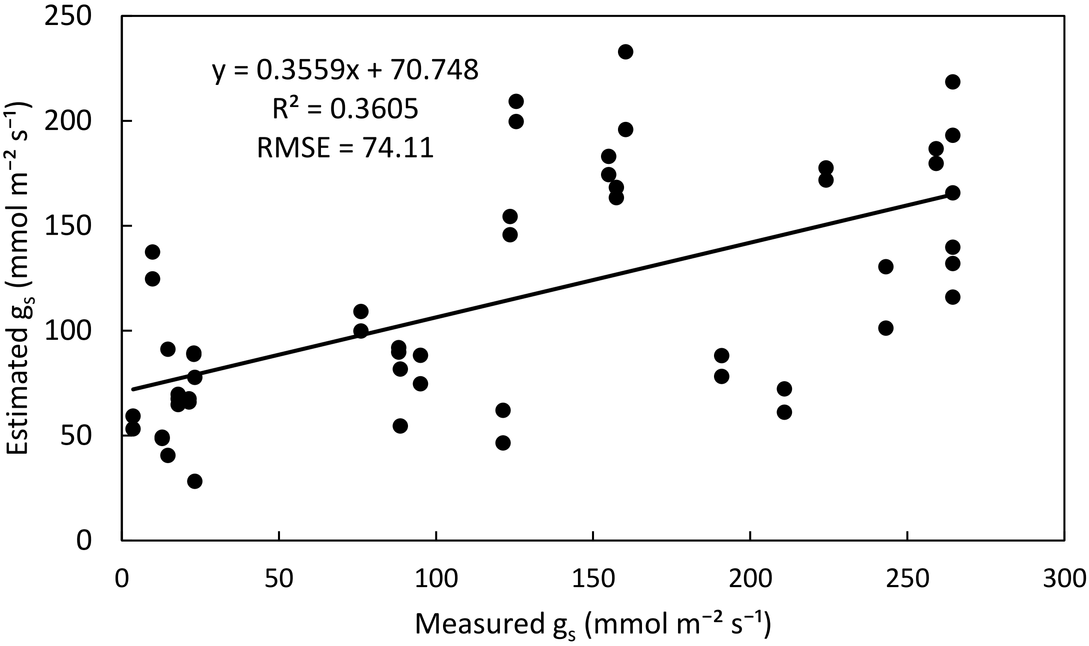

Figure 4
Relationship between g_S measured using a porometer and estimated g_S based on leaf spectral reflectance collected by the SCiO for Cabernet Sauvignon.

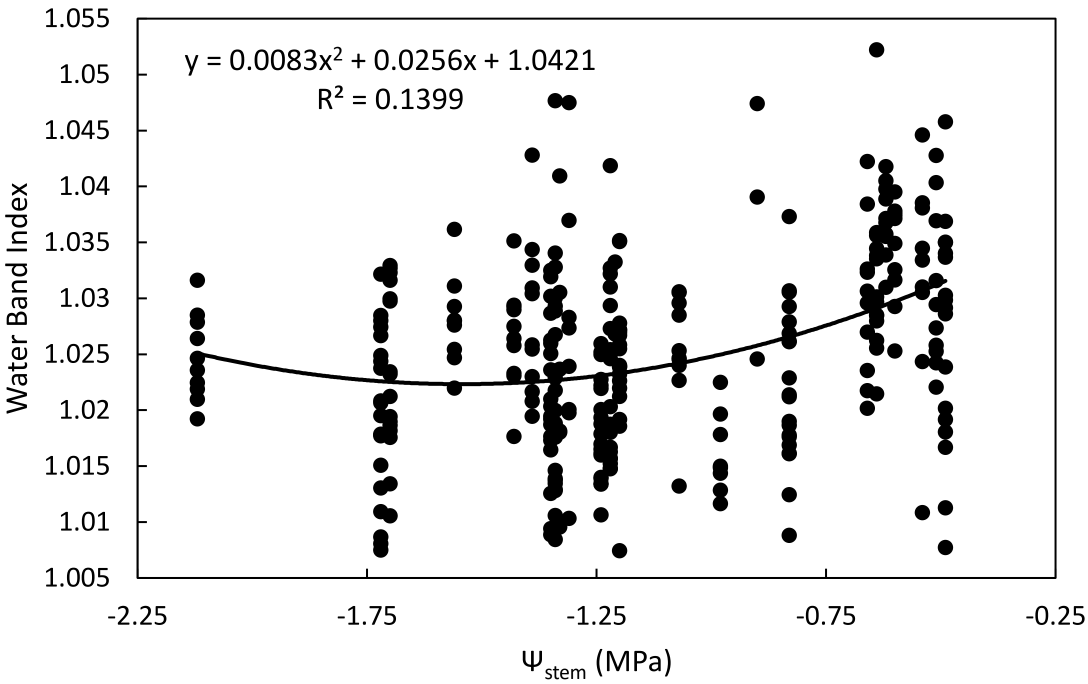

Figure 5
The relationship between the Ψ_{stem} measured using a pressure chamber and Water Band Index (reflectance at 970nm/900nm) measured using the SCiO for Cabernet Sauvignon and Chardonnay.

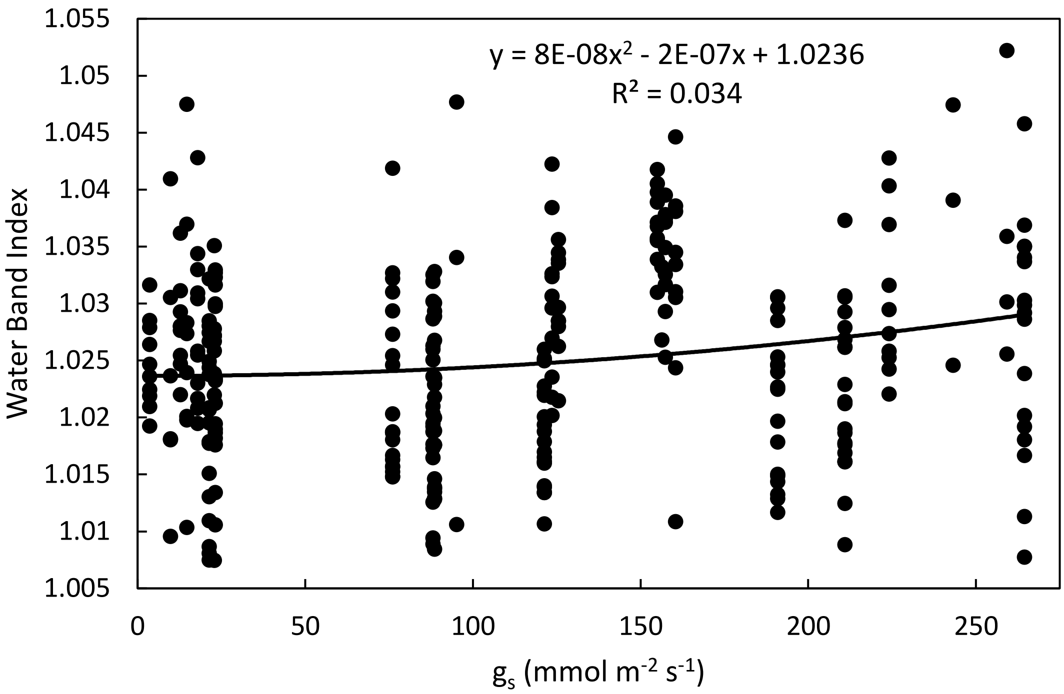

Figure 6
The relationship between g_S measured using a porometer and Water Band Index (reflectance at 970nm/900nm) measured using the SCiO for Cabernet Sauvignon and Chardonnay.

Stomatal aperture

Despite trialling three models of smartphone compatible microscopes; we were unable to directly collect images of suitable resolution and clarity in the field to allow the stomatal density and aperture to be analysed directly. While the stomata could be distinguished in the best example images (Figure 7), we struggled to collect images of this quality consistently in the vineyard. As an alternative, while higher resolution microscopes were being investigated, we collected and analysed stomatal peels. The analysis of images of stomata impressions in nail polish proved successful with a precision of over 90% recorded for test images. This was better than the 50-60% precision seen by other authors, and further details are presented in Jayakody et al. (2017), please refer to the Communications section. Unfortunately, until microscopes with higher resolution and better lighting systems are available for mounting on smartphones, this technique is not practical for field use.

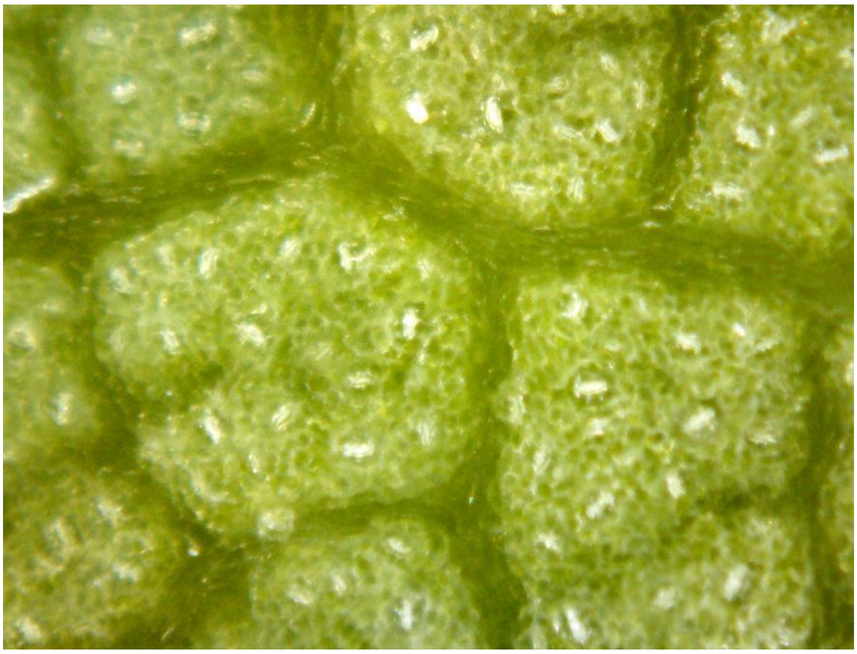

Figure 7
Example image of stomata on the underside of a grapevine leaf collected with a ProScope HR2. This image was collected in the laboratory under ideal conditions.

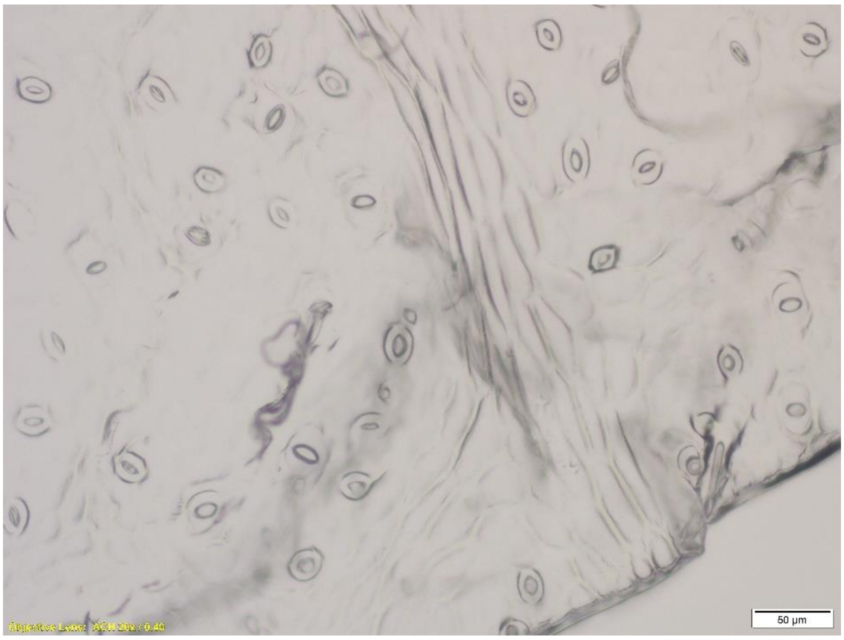

Figure 8
Example image of a stomatal peel collected using nail polish applied to a leaf and then photographed on a binocular microscope.

3D Camera based leaf angle

The scale-invariant feature technique (SIFT) used to determine sparse correspondences between the stereo leaf images failed to detect the leaves in this situation (Figure 9). The uniform black background was effectively featureless, meaning its position with respect to the camera could not be accurately characterised. The leaf itself was also relatively featureless, hence very few points on the surface could be correlated between the images and then used to obtain depth values that would have been an indication of cupping. While the

chequerboard pattern provided clear features, it does not contribute to measurement of the leaf. Hence this method was not effective for measuring leaf shape.
An alternative method to estimate leaf shape using structure from motion was also tested. This generated a 3D point cloud for each leaf (Figure 10); the missing segments of the leaf are due to homogeneous surface textures causing the matching to be inaccurate (Zhang et al. 2016). This process was also computationally expensive, taking several minutes per leaf as it employs a global matching algorithm. Unfortunately, when the leaves were profiled, the amount of cupping that was detected was quite small, even on the severely water stressed treatments (Figure 10). This suggests that insufficient differentiation between stressed and unstressed leaves could be observed by analysing the amount of leaf cupping.

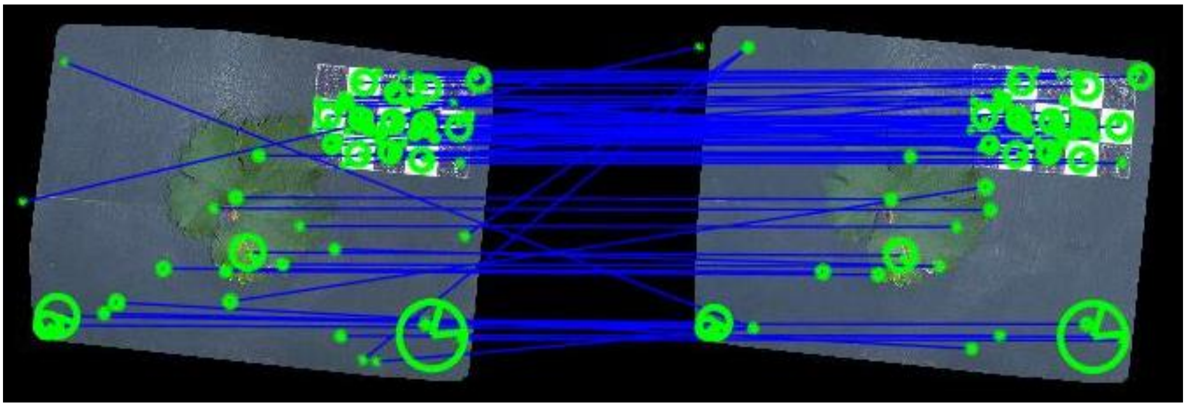

Figure 9
Scale-Invariant Feature Transform feature matching between stereo images, showing lack of features detected on leaf.

Figure 10
Front (left) and side (right) view of the leaf image generated using dense stereo matching, note the very limited variation in depth in the side view image.

Thermal imaging – Season 1

Of the two smartphone based thermal camera systems used, the FLIR™ One provided images that were clear and easier to interpret compared to the Seek (Figure 10 and Figure 11). This meant that the temperatures of wet and dry reference surface temperatures were significantly easier to extract from the FLIR™ One images compared to the Seek images. The resolution of the professional thermal camera (FLIR 365) was significantly better than either of the smartphone based cameras (Figure 12), however the cost of these cameras is up to 100 times the smartphone based systems and they do not contain the onboard processing capability to analyse the image and estimate water stress.

The CWSI was calculated based on the $T_{canopy,}$ $T_{wet(leaf)}$ and $T_{dry(leaf)}$. When these calculations were compared to the reference methods, Ψ_{stem} (Figure 14) and g_S (Figure 15), they gave the most consistent and robust results. Therefore, this method was developed further during the second season to confirm its accuracy and utility.

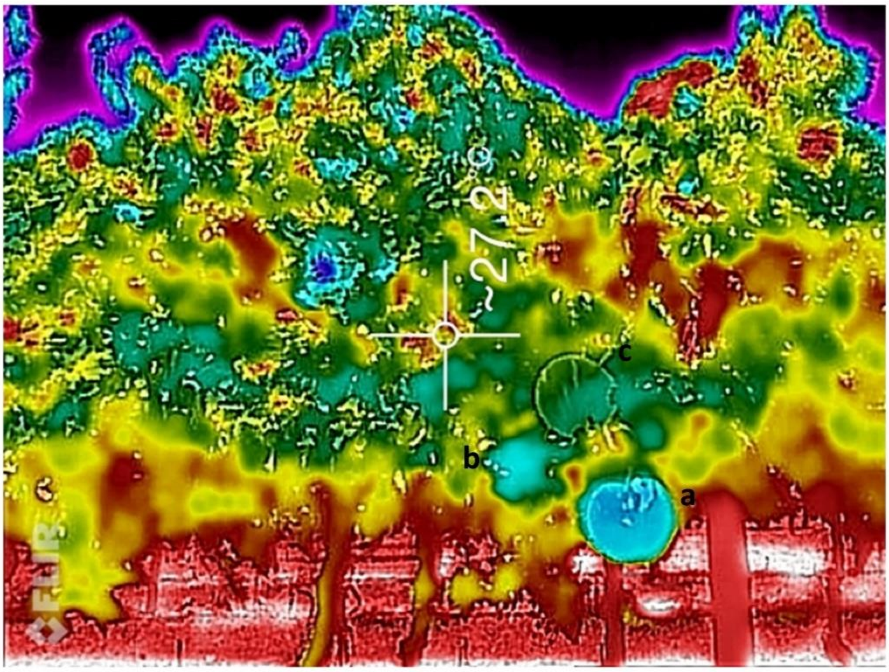

Figure 11
Thermal image collected by the FLIR One camera, note the outline provided by the RGB camera which makes the thermal camera easier to orientate. (a) represents wet filter paper, (b) represents a wet leaf and (c) represents dry filter paper.

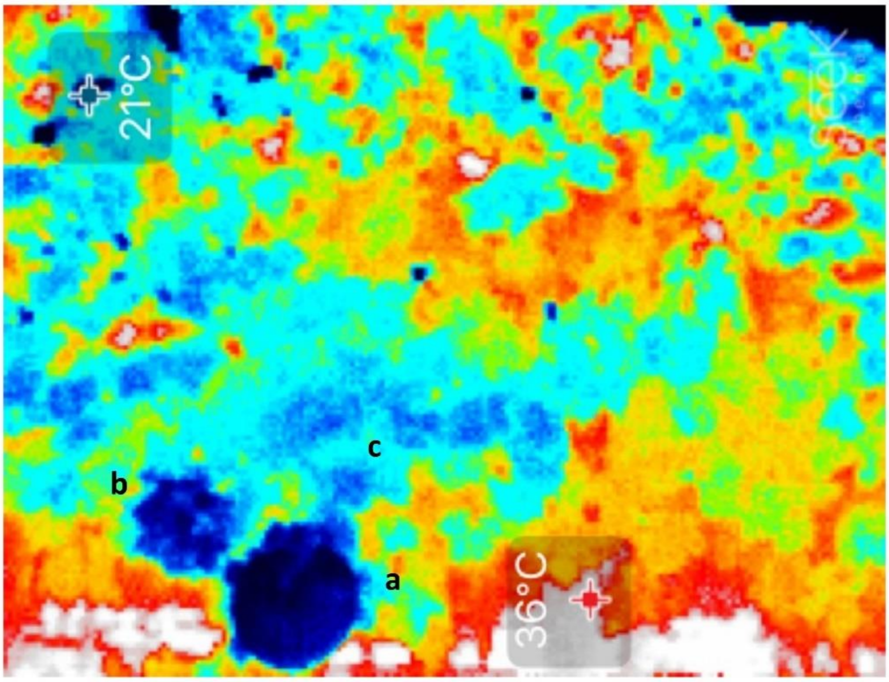

Figure 12
Thermal image collected by the Seek camera. (a) represents wet filter paper, (b) represents a wet leaf and (c) represents dry filter paper.

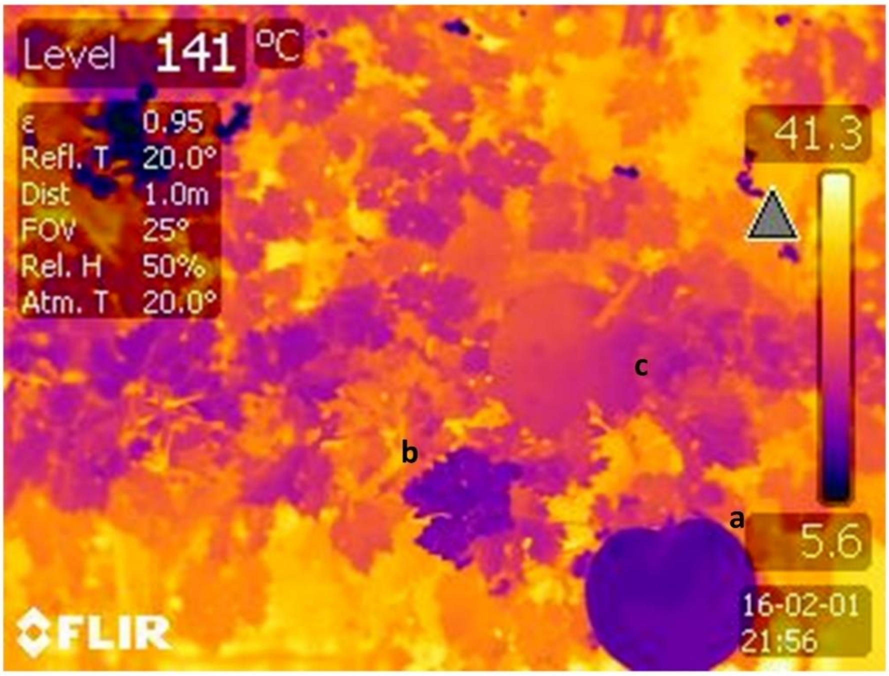

Figure 13
Thermal image collected by the FLIR 365B camera, note the higher resolution provided by a professional camera. (a) represents wet filter paper, (b) represents a wet leaf and (c) represents dry filter paper.

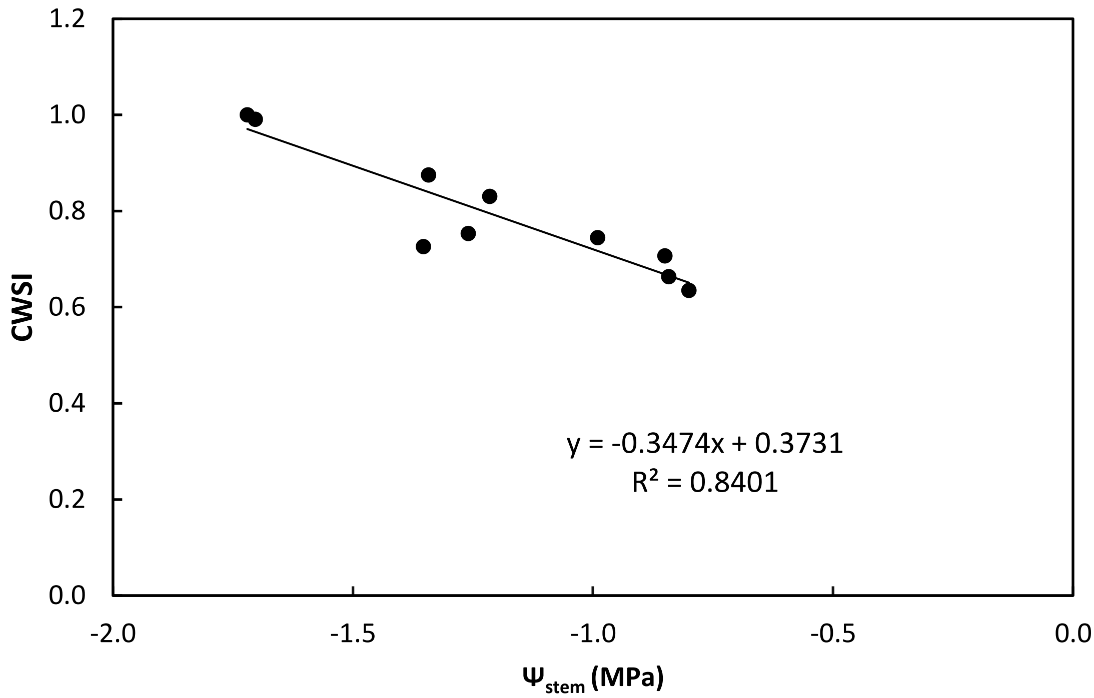

Figure 14
The relationship between Ψ_{stem} and CWSI as assessed during the 2015-16 growing season. Results were collected from both Cabernet Sauvignon and Chardonnay (see methods for more details of the plant material).

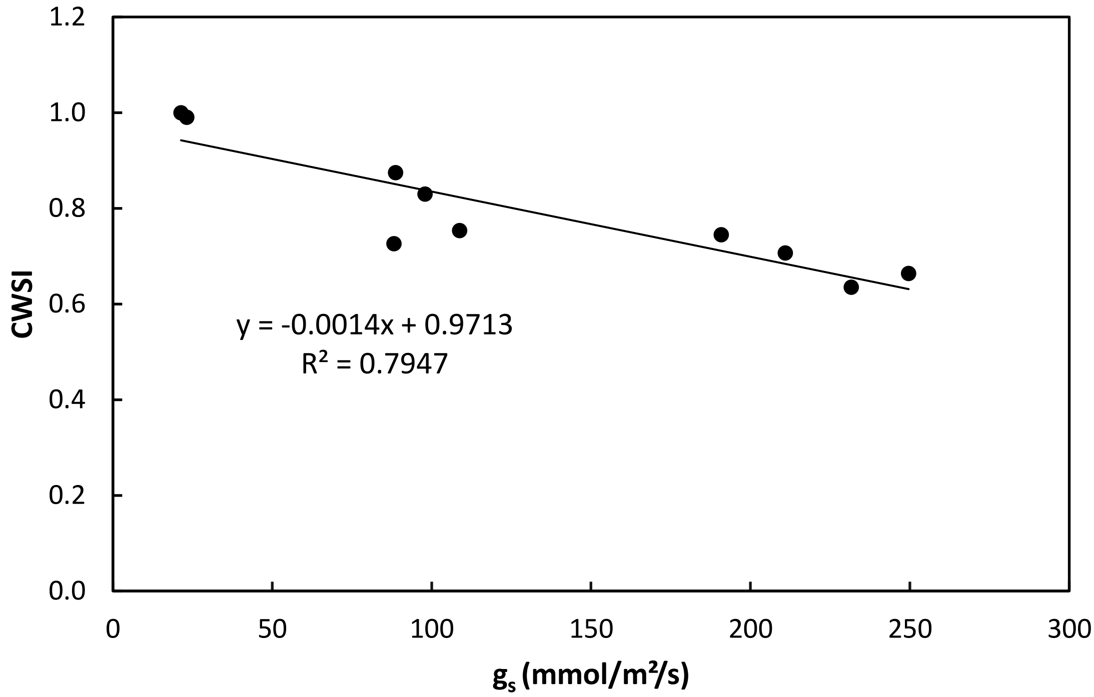

Figure 15
The relationship between g_S and CWSI as assessed during the 2015-16 growing season. Results were collected from both Cabernet Sauvignon and Chardonnay (see methods for more details of the plant material).

Thermal imaging – Season 2

The selection of the canopy, so that T_{canopy} can be determined, and the accurate assessment of T_{dry} and T_{wet} are critical to the calculation of g_s and the water stress indices. The application appeared to accurately select the canopy and the T_{dry} and T_{wet} in almost all cases (e.g. Figure 16). The reliability of the canopy selection was assessed by comparing canopy temperatures calculated from a manually selected portion of the canopy and the fully automated selection. A strong, 1:1 relationship, was seen between the manually selected section of the canopy and the fully automated method (Figure 17), this gave us confidence in the methods used to select the canopy.

A second assessment was completed to determine the accuracy of using artificial T_{dry} and T_{wet} as substitutes for leaves treated with sprayed water or petroleum jelly. The temperature of the $T_{dry(pet)}$ was used as the benchmark comparison to the temperature of the $T_{dry(fab)}$ and the $T_{dry(leaf)}$. A strong relationship was seen between the $T_{dry(pet)}$ and both the $T_{dry(fab)}$ and the $T_{dry(leaf)}$ (Figure 18 and Figure 19), however, this relationship was not 1:1 in either case. The relationship between $T_{wet(leaf)}$ and $T_{wet(fab)}$ was not as strong as between the dry temperature references, however the R^2 was above 0.87 and once again, the slope was not 1:1 (Figure 20). As the relationship between the leaf and the fabric based T_{dry} and T_{wet} was not 1:1, a correction factor was developed for use prior to the calculation of the indices so that the values were equivalent to those collected from the $T_{wet(leaf)}$ and $T_{dry(leaf)}$.

Indices calculated from the canopy temperature were compared to g_S (Figure 21, Figure 22, Figure 23, Figure 24 and Figure 25) and Ψ_{stem} (Figure 26, Figure 27, Figure 28, Figure 29, Figure 30). The relationships between $g_{S(porometer)}$ and the indices was linear, while the relationships between Ψ_{stem} and the indices was best predicted using a curvilinear model. The CWSI showed the strongest relationships with both $g_{S(porometer)}$ and Ψ_{stem} (Figure 21 and Figure 26) and the relationship between $g_{S(porometer)}$ and the index was always stronger than the relationship between Ψ_{stem} and the equivalent index. This assessment confirmed that the CWSI was the best option for the assessment of vine water stress under the test conditions.

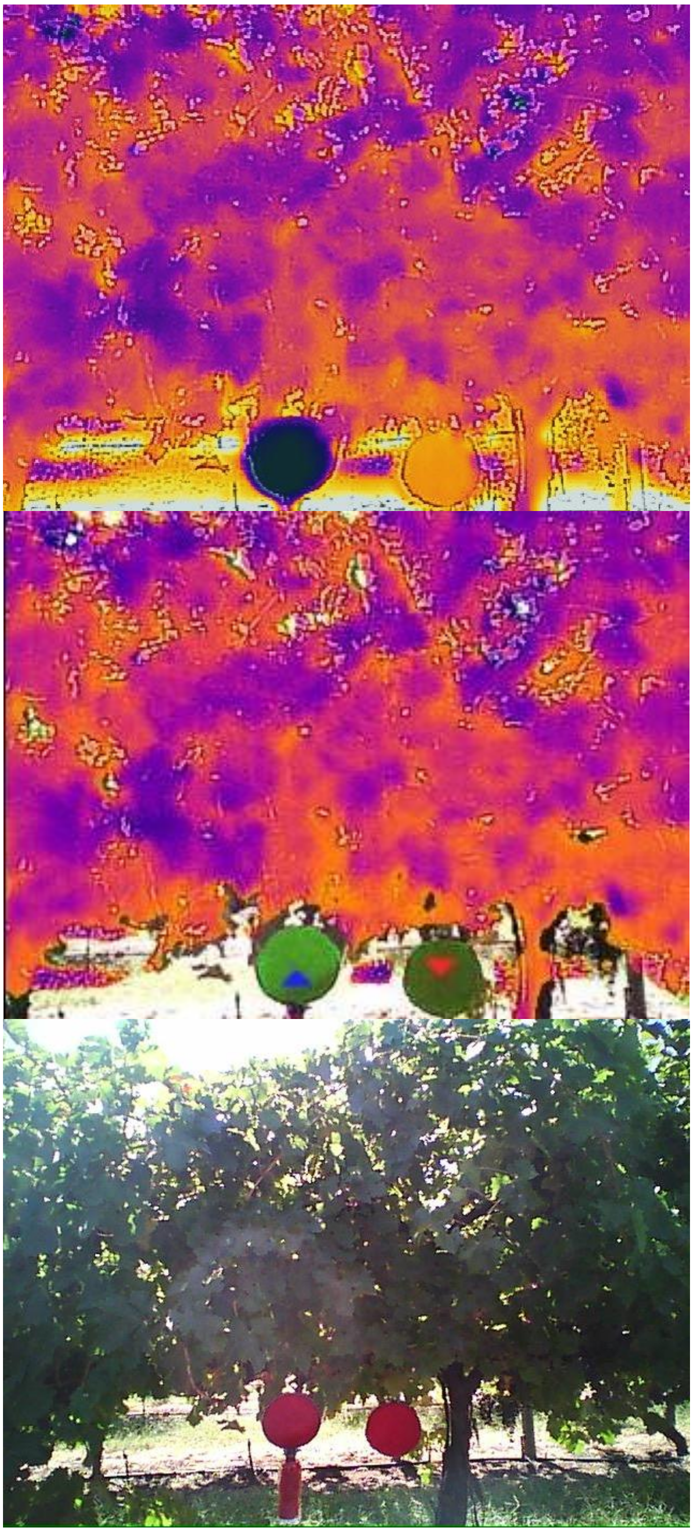

Figure 16
Thermal image as collected by the FLIR One (top). A screen shot of image as displayed by the application showing the canopy demarcated using the thermal colours, the reference surfaces as green and the warmest and coolest points on the reference surfaces as the blue and red triangles respectively (centre). The RGB image of the canopy as collected by the VGA camera on the FLIR One (bottom).

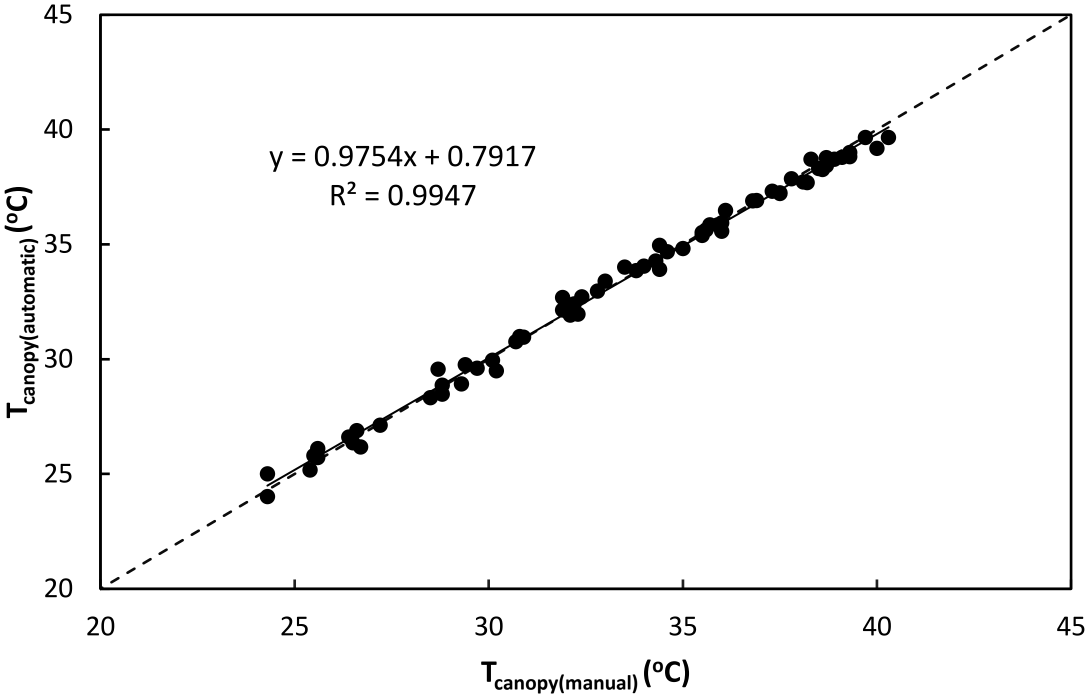

Figure 17
The relationship between the temperature of a manually selected section of the grapevine canopy ($T_{canopy(manual)}$) and the temperature of the entire canopy selected automatically by the application ($T_{canopy(automatic)}$). Dashed line is 1:1.

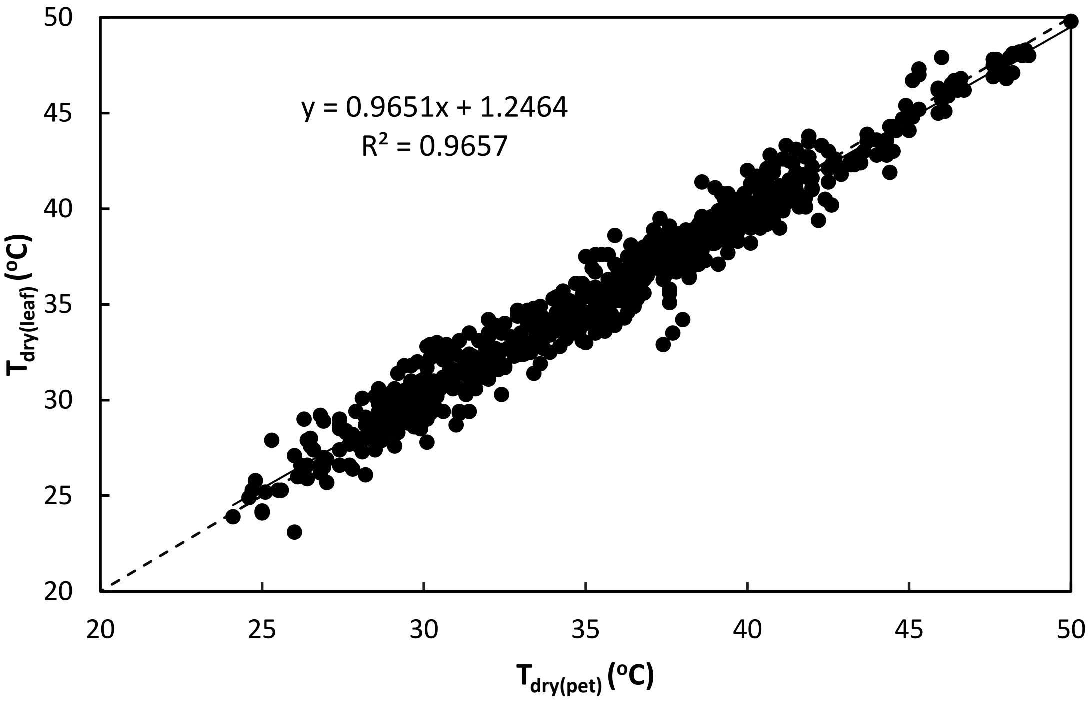

Figure 18
The relationship between the temperature of the leaf with the abaxial side coated with petroleum jelly ($T_{dry(pet)}$) and the temperature of a detached leaf ($T_{dry(leaf)}$) that was suspended in the canopy. Dashed line is 1:1.

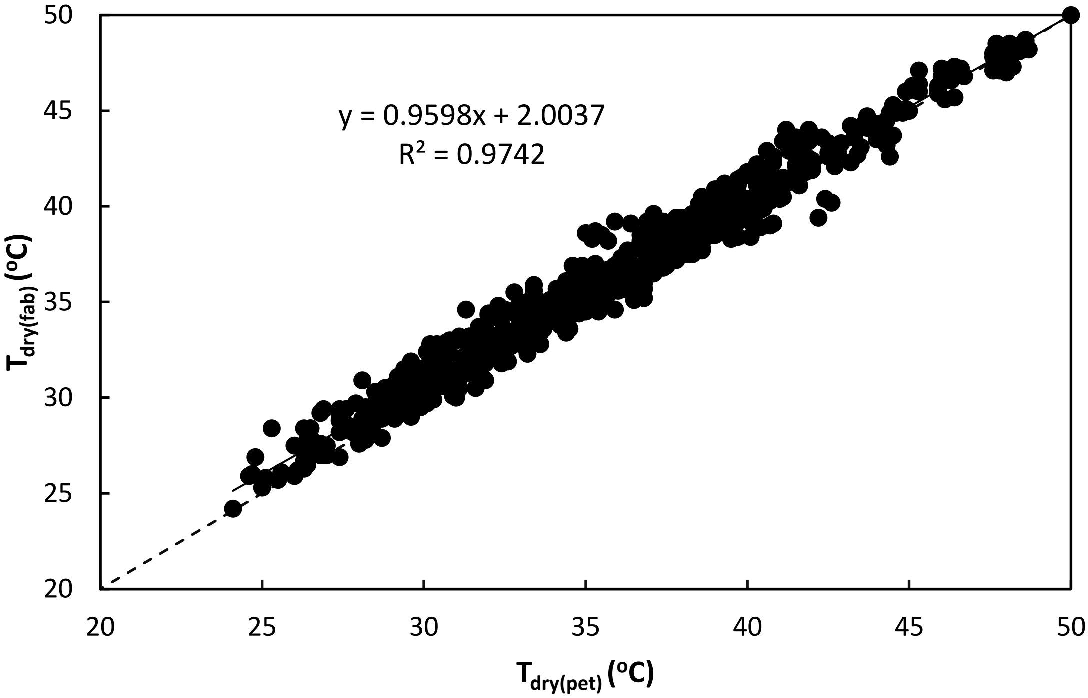

Figure 19
The relationship between the temperature of the leaf with the abaxial side coated with petroleum jelly ($T_{dry(pet)}$) and the temperature of a fabric reference ($T_{dry(fab)}$) that was suspended in the canopy. Dashed line is 1:1.

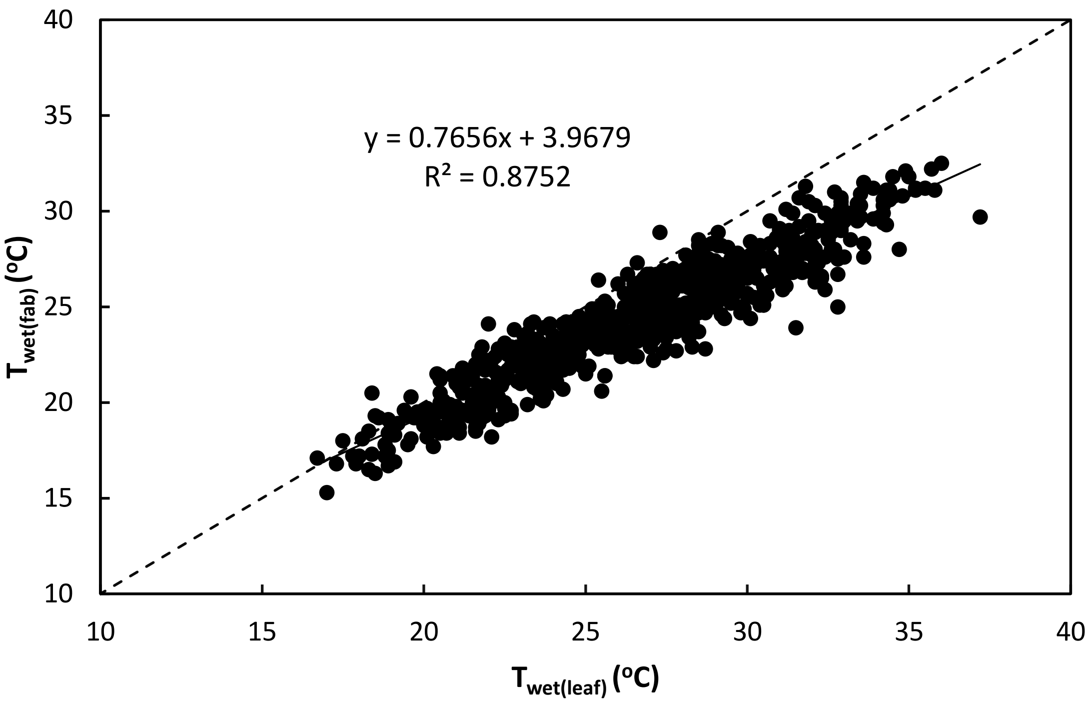

Figure 20
The relationship between the temperature of the leaf where the adaxial surface had been sprayed with water ($T_{wet(leaf)}$) and the wet fabric reference surface ($T_{wet(fab)}$). Dashed line is 1:1.

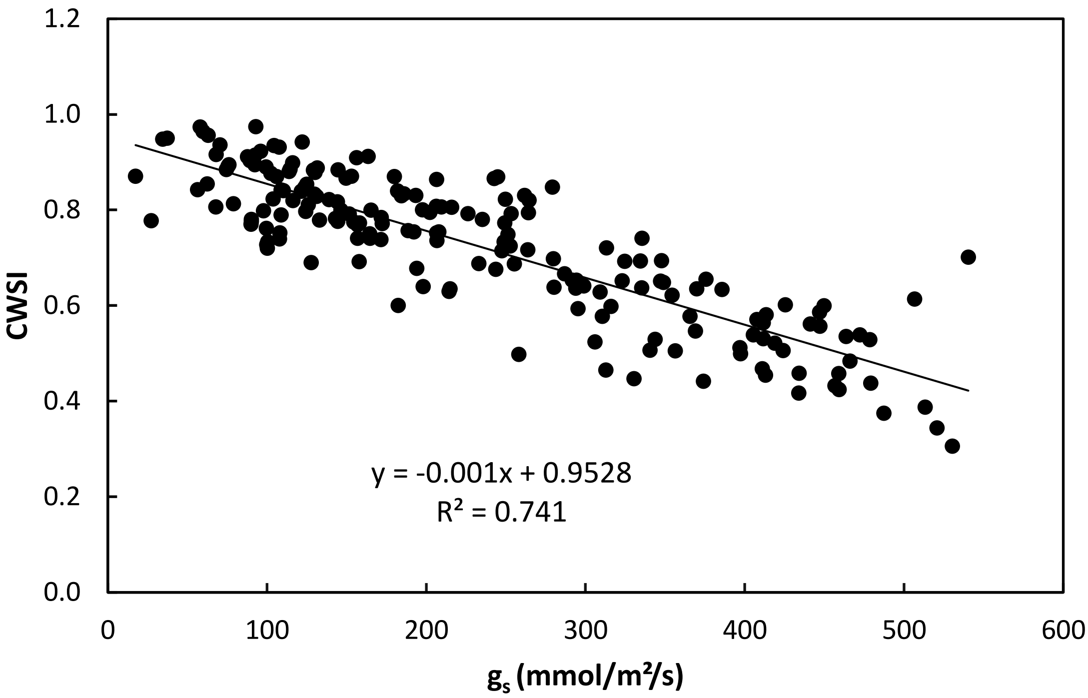

Figure 21
The relationship between g_S of Chardonnay and Cabernet Sauvignon subject to a range of water deficit treatments (see text for details) and CWSI calculated from the average canopy temperature and the wet ($T_{wet(fab)}$) and dry ($T_{dry(fab)}$) fabric reference surfaces.

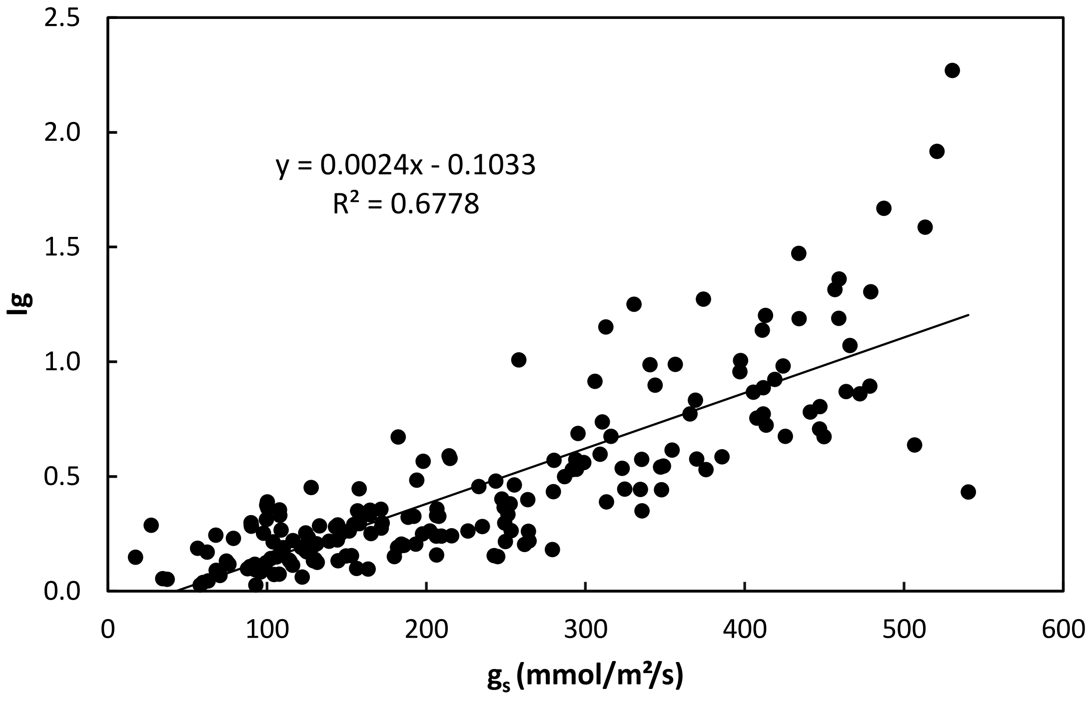

Figure 22
The relationship between g_S of Chardonnay and Cabernet Sauvignon subject to a range of water deficit treatments (see text for details) and Ig calculated from the average canopy temperature and the wet ($T_{wet(fab)}$) and dry ($T_{dry(fab)}$) fabric reference surfaces.

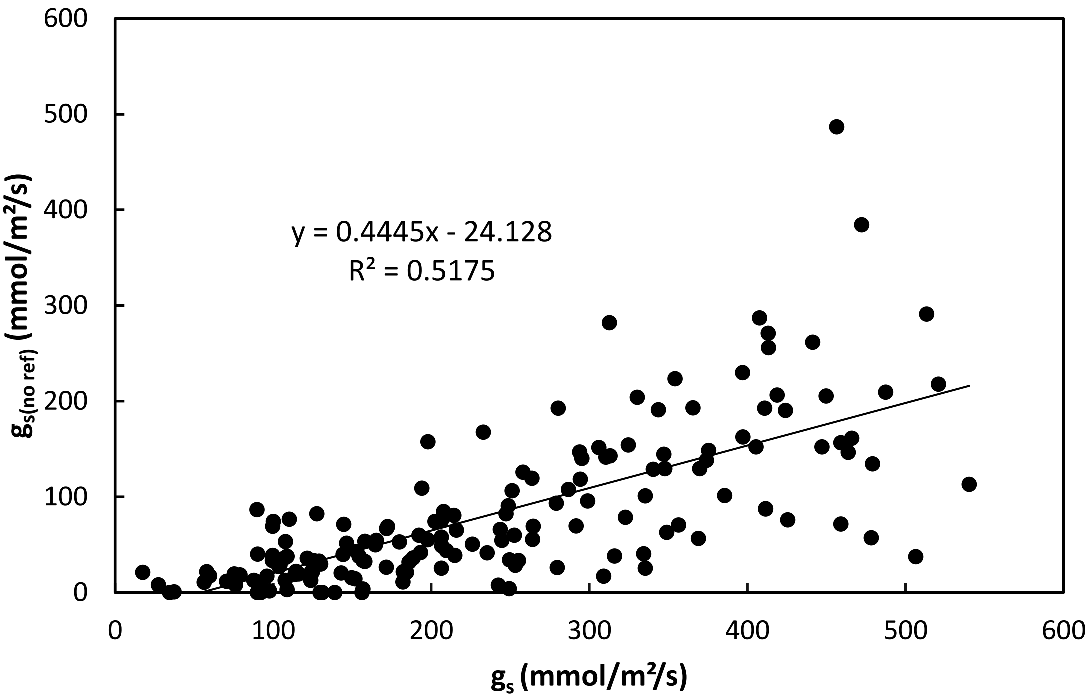

Figure 23
The relationship between *gS* of Chardonnay and Cabernet Sauvignon subject to a range of water deficit treatments (see text for details) and $g_{s(\text{no ref})}$ calculated from the average canopy temperature and environmental parameters (see text for details).

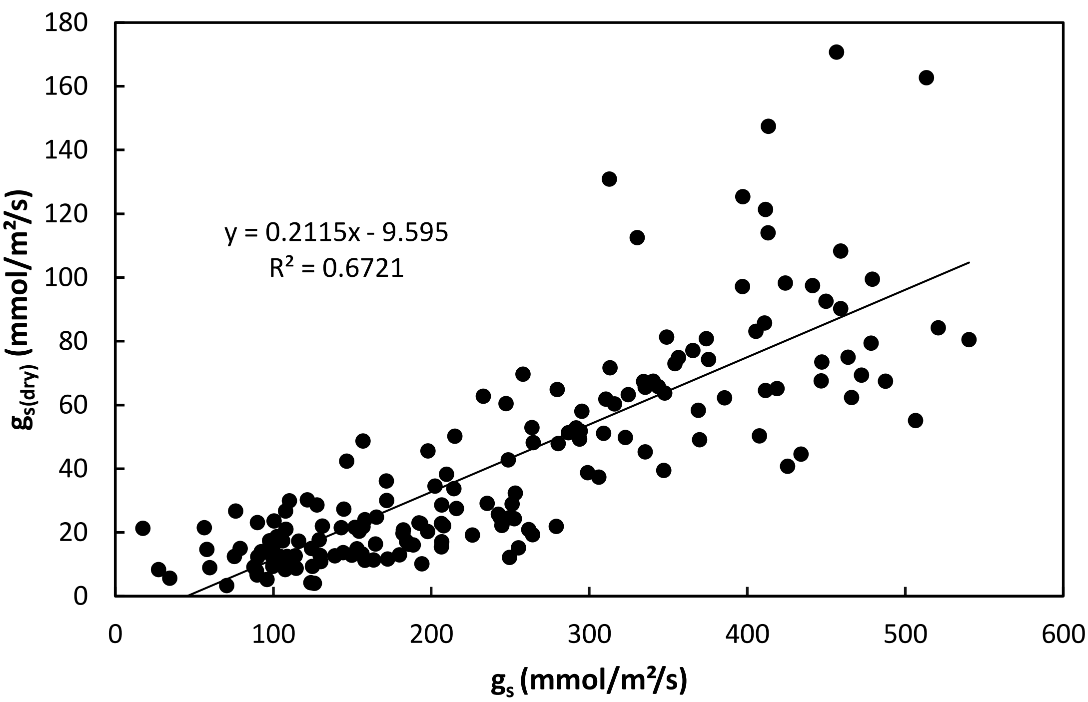

Figure 24
The relationship between *gS* of Chardonnay and Cabernet Sauvignon subject to a range of water deficit treatments (see text for details) and $g_{s(\text{dry})}$ calculated from the average canopy temperature, environmental parameters and the dry fabric reference ($T_{\text{dry(fab)}}$).

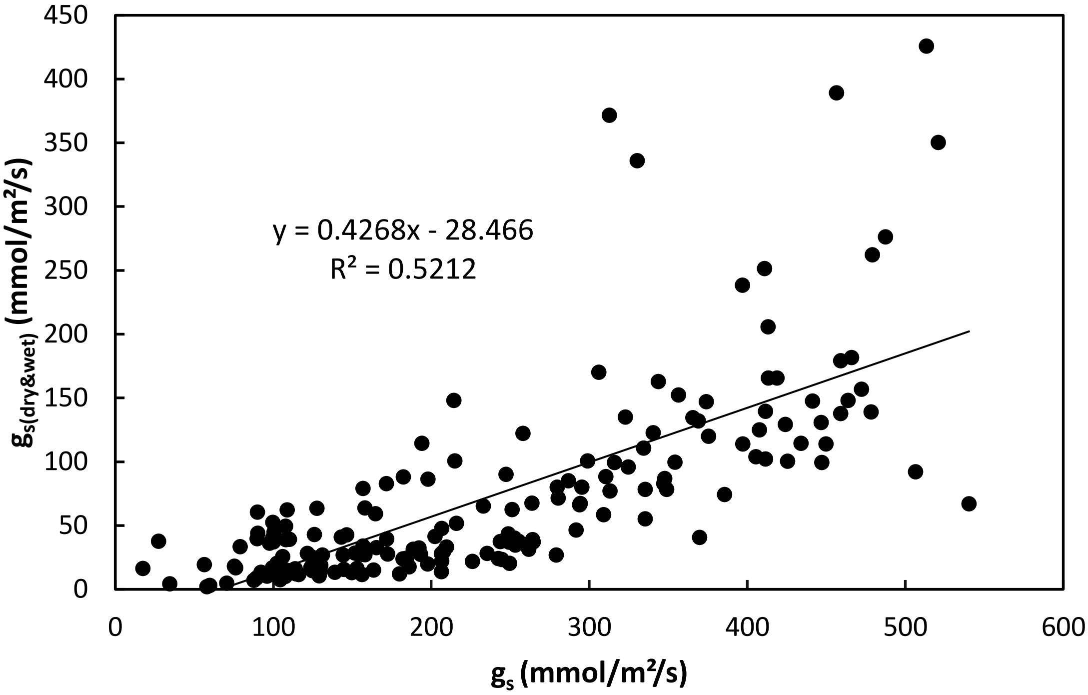

Figure 25
The relationship between g_S of Chardonnay and Cabernet Sauvignon subject to a range of water deficit treatments (see text for details) and $g_{s(dry\&wet)}$ calculated from the average canopy temperature, environmental parameters and the wet ($T_{wet(fab)}$) and dry ($T_{dry(fab)}$) fabric reference.

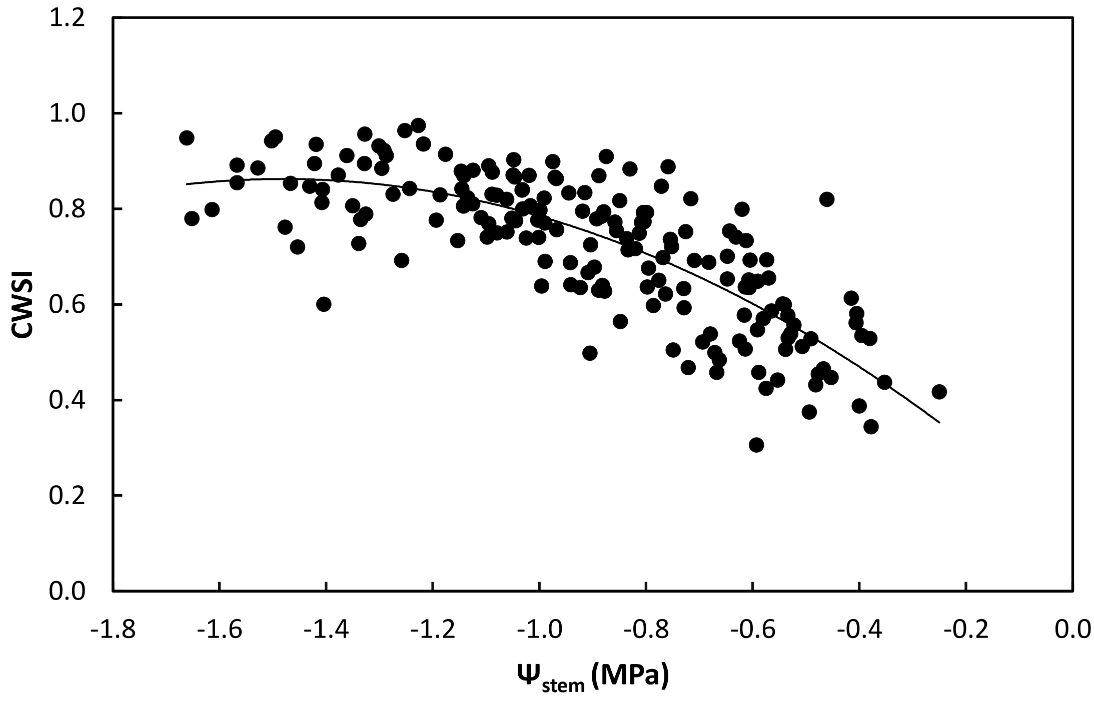

Figure 26
The relationship between Ψ_{stem} averaged from three leaves of Chardonnay and Cabernet Sauvignon subject to a range of water deficit treatments (see text for details) and CWSI calculated from the average canopy temperature and the wet ($T_{wet(fab)}$) and dry ($T_{dry(fab)}$) fabric reference.

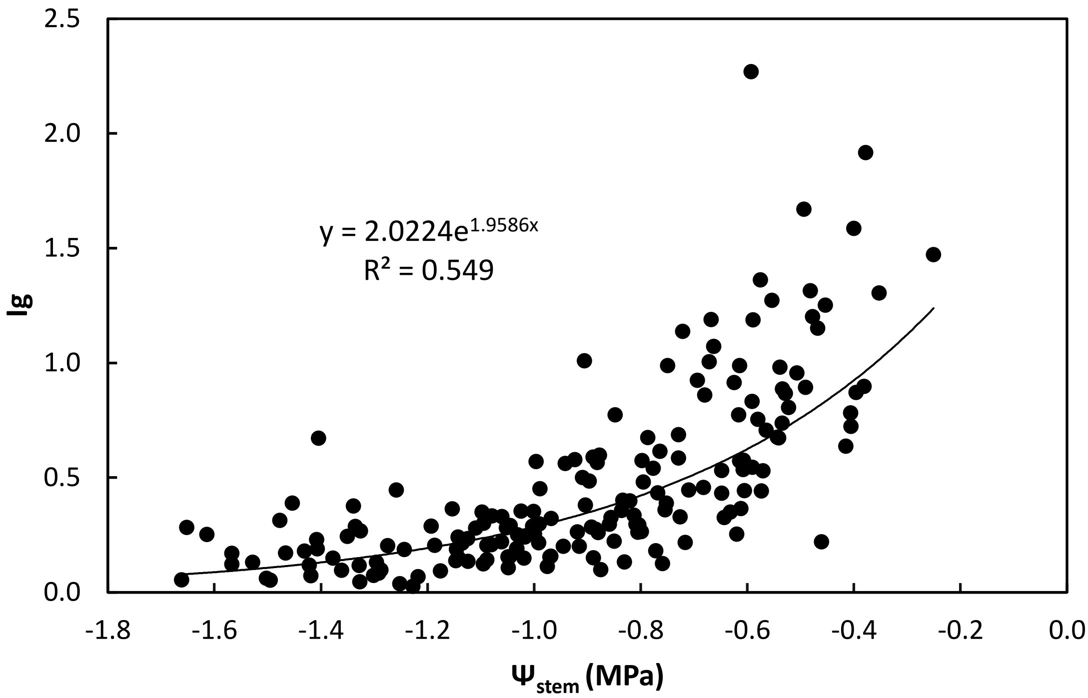

Figure 27
The relationship between Ψ_{stem} averaged from three leaves of Chardonnay and Cabernet Sauvignon subject to a range of water deficit treatments (see text for details) and conductance index (Ig) calculated from the average canopy temperature and the wet ($T_{wet(fab)}$) and dry ($T_{dry(fab)}$) fabric reference surface.

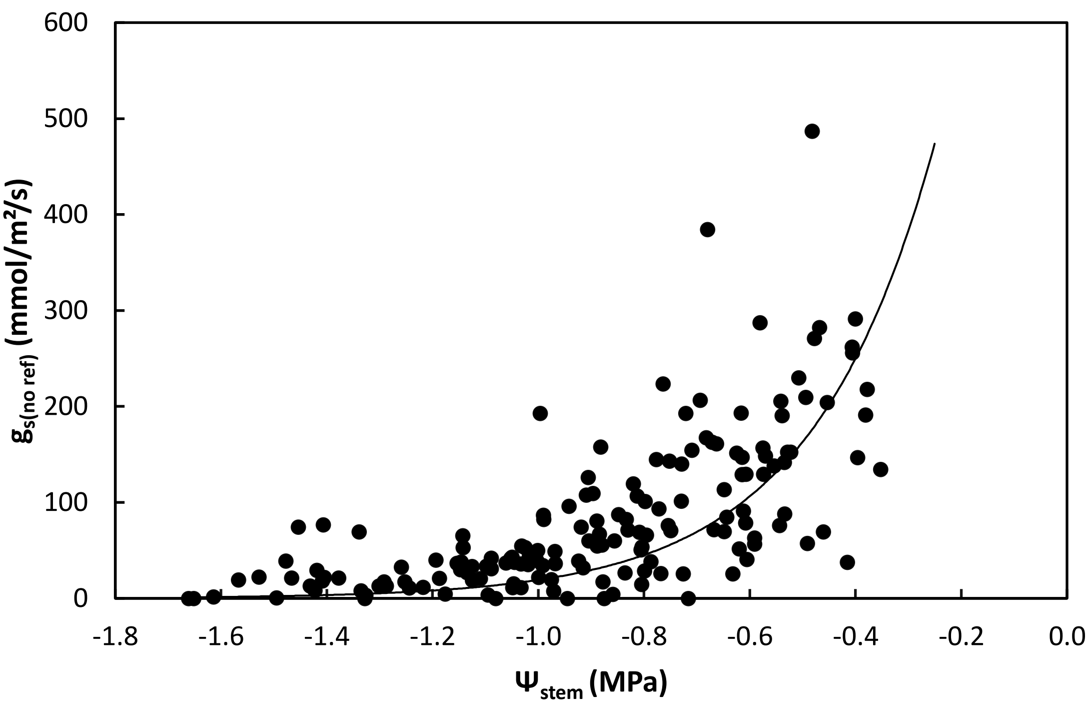

Figure 28
The relationship between Ψ_{stem} averaged from three leaves of Chardonnay and Cabernet Sauvignon subject to a range of water deficit treatments (see text for details) and $g_{s(no\ ref)}$ calculated from the average canopy temperature and environmental parameters.

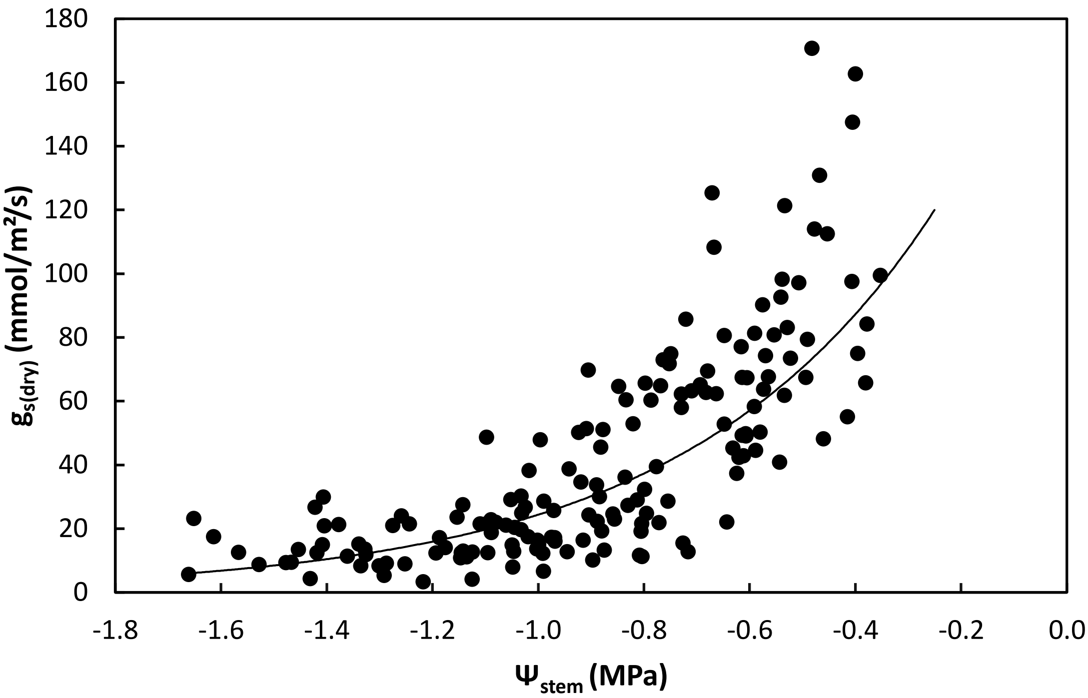

Figure 29
The relationship between Ψ_{stem} averaged from three leaves of Chardonnay and Cabernet Sauvignon subject to a range of water deficit treatments (see text for details) and $g_{s(dry)}$ calculated from the average canopy temperature, environmental parameters and the dry fabric reference ($T_{dry(fab)}$).

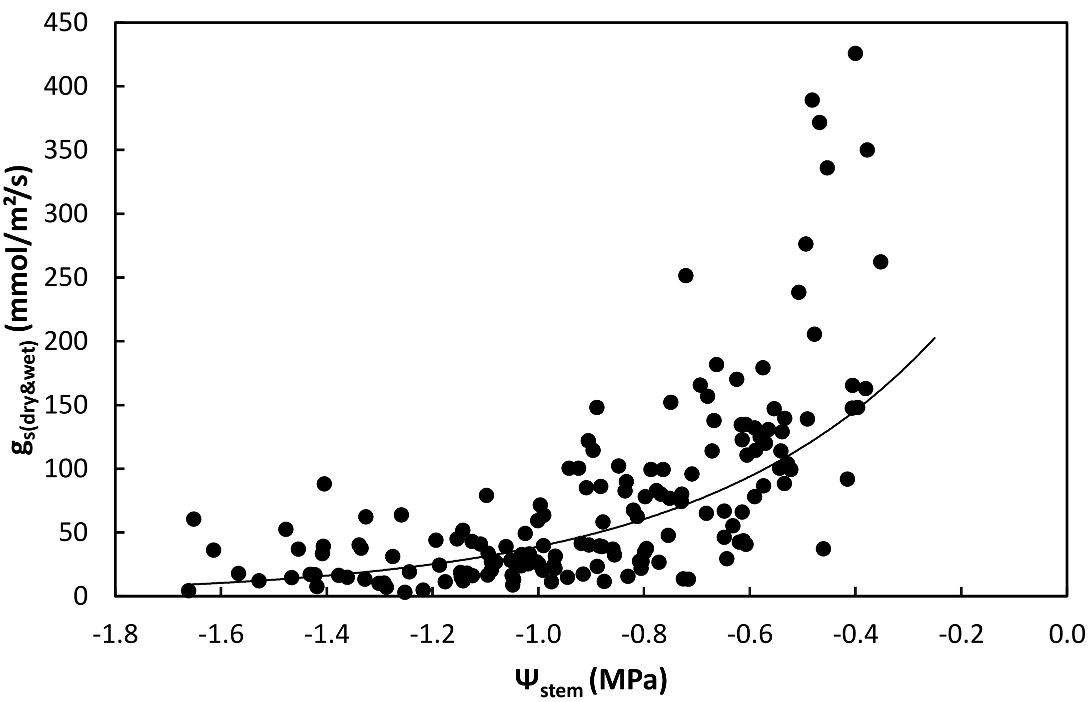

Figure 30
The relationship between Ψ_{stem} averaged from three leaves of Chardonnay and Cabernet Sauvignon subject to a range of water deficit treatments (see text for details) and $g_{s(dry\&wet)}$ calculated from the average canopy temperature, environmental parameters and the wet ($T_{wet(fab)}$) and dry ($T_{dry(fab)}$) fabric reference.

User acceptance testing

Most users found the application simple to use and the instructions (Appendix 5) easy to follow. They generally felt that the results (CWSI) reflected the appearance of the vines or their other measurements of water status (primarily soil moisture content) (Table 1). Comments suggested that the unusually wet season in some locations meant that vines did not experience the usual level of water stress, which limited some of the opportunities to test the application (Appendix 5). There was less certainty about the utility of the CWSI for scheduling irrigation, but none of the testers disagreed with this question (Table 1). Comments from the interviews suggested that once the users became more familiar with the application and the CWSI as a method for assessing vine water status, the confidence in this technique would improve (Appendix 5). The primary areas of concern for the testers were the need to collect images from the shaded side of the row and the requirements to erect the $T_{dry(fab)}$ and $T_{wet(fab)}$ in the canopy for each reading (Appendix 5). Several users suggested improvements to the mounting or display of the $T_{dry(fab)}$ and $T_{wet(fab)}$ which are easy to implement. Others requested that a system be developed that does not require the reference surfaces. These methods were investigated further as part of this project (see above). Over 80% of the testers would consider using the application in the future and recommend it to others to use (Table 1).

Table 1
Responses of beta testers to statements regarding the performance of the application and questions on intentions for future use.

	Strongly Disagree	Disagree	Neutral	Agree	Strongly Agree
The App was simple to use	0 %	0 %	0 %	75 %	25 %
The methodology for using the app is clearly defined in the instructions	6 %	0 %	13 %	56 %	25 %
I was comfortable installing the reference leaves for each set of measurements	13 %	6 %	25 %	50 %	6 %
The CWSI results were what you expected	6 %	0 %	19 %	63 %	13 %
I considered the weather conditions when making measurements and interpreting results	0 %	6 %	19 %	38 %	38 %
The CWSI figures were useful in making irrigation decisions	0 %	0 %	38 %	50 %	13 %
Would you consider using the app in the future?	13 %	n/a	6 %	n/a	81 %
Would you recommend the app to others?	0 %	n/a	12.5 %	n/a	88 %

Outcomes and conclusions

This project has successfully evaluated a range of smartphone based methods to assess vine water stress quickly and easily in the vineyard. The most promising method was selected, and this was developed into a prototype smartphone application. The app was tested to demonstrate its accuracy and confirm that the most appropriate indices were being used. It was also beta tested by viticulturists to assess its utility with further improvements being made based on this testing. These were the broad objectives established in the project proposal.

An easy, portable and cost-effective system for the direct and real-time assessment of plant water status remains a challenge for all agricultural industries. The system developed as part of this project offers the potential to meet these requirements. Traditionally the Australian industry has relied on soil moisture monitoring as it can give a direct measure of soil content and its relatively slow changes in response to rainfall, irrigation and water use by the vines. Plant based methods of assessing water status in contrast are often far more dynamic in response to the environment. They integrate the amount of moisture available in the soil with the environmental conditions to indicate how stressed the vine is ‘feeling’. Sudden changes in the environment such as an increase in wind or cloud cover can rapidly impact on these results. The CWSI is a direct measurement of the vine’s water status. This is a benefit as you can assess how the vine is ‘feeling’, based on the weather conditions as well as how much moisture is in the soil. It can also be a drawback as transient changes in conditions, such as scattered cloud, can influence the results; potentially increasing the variation between measurements.

There is a range of scenarios in which CWSI could be used to inform irrigation scheduling that could complement or replace existing soil moisture monitoring systems. Regular assessment of the CWSI in a vineyard will help develop an understanding of what values to expect from different blocks or varieties. If the target is to maximise vineyard yield then water stress needs to be avoided, while not applying excessive water. Checking the CWSI immediately prior to applying irrigation would confirm that no stress had occurred. Preliminary estimates suggest that a CWSI of less than 0.7 recorded from a shaded canopy on a hot day, or 0.5 on a cooler day would indicate vines are well irrigated. If the target is to optimise quality and minimise water use as part of a regulated deficit irrigation strategy, then the CWSI could also be used to inform irrigation decisions. If the vines are being maintained at a moderate water deficit (for example during the post flowering period) then irrigation could be withheld if the CWSI is below approximately 0.8 assuming very hot weather is not forecast. Tracking the CWSI over time may give a viticulturist more confidence to extend the period between irrigation applications. Soil moisture monitoring systems are normally point based at a limited number of sites across a vineyard; it is uncommon for all the blocks within a vineyard to be covered. The thermal camera is very portable and can be used to compare different parts of a block and across blocks. This system provides an easy opportunity to check sections of a block that may not be receiving enough water, and benchmark these against the section adjacent to the soil moisture probe.

If the app is developed further and maintained so that it can be used by the wine industry, then the savings in water applications are likely to occur as growers will be able to more easily assess if their blocks require irrigation. Fruit quality will also potentially be improved, through the better management of regulated water deficit, and by applying strategic irrigations to maintain canopy health and avoid defoliation.

Recommendations

The application should be developed from a prototype to a commercial system with initial support for three growing seasons so the uptake by industry can be assessed. Currently only broad recommendations on the optimum CWSI values for specific target outcomes are available. These targets are likely to vary between cultivars, wine styles and regions; and most growers will want to select and refine the target CWSI values to meet their needs. If the lack of specific recommendations on CWSI becomes an impediment to uptake, then regional associations could be supported to develop their own benchmarking programs.

Appendix 1: Communication

Articles

Jayakody, H., Liu, S., Whitty, M., and Petrie, P. (2017) Microscope image based fully automated stomata detection and pore measurement method for grapevines. Plant Methods 13, 94.

Liu S, Tang J, Petrie P, and Whitty M. A Fast Method to Measure Stomatal Aperture by MSER on Smart Mobile Phone (2016), Applied Industrial Optics: Spectroscopy, Imaging and Metrology 2016, Heidelberg, Germany, 25 - 28 July 2016.

Skewes, M., Petrie, P., Liu, S., and Whitty, M. (2018) Smart Phone Tools for Measuring Vine Water Status Acta Horticulturae, In Press

Skewes, M. (2017) Smart phone tool measures vine water status. Irrigation Australia, 33, 13-14.

Presentations

Petrie, P., Skewes, M., Wang, M., Whitty, M., Lam, S., and Liu, S. (2017) A Thermal Camera Based Smartphone Application to Measure Vine Water Status, American Society for Viticulture and Enology 68th Annual Meeting, Bellevue, Washington, USA, 26-29 June 2017.

Skewes M, Liu S, Petrie P, and Whitty MA. Smart Phone Tools for Measuring Vine Water Status, (2016) International Symposium on Sensing Plant Water Status, Potsdam, Germany, 5-7 October 2016.

Skewes, M., Wang, M., Whitty, M., Lam, S., Petrie, P. and Liu, S. Smart Phone Assessment of Water Stress, (2017) Intelligent Systems – Profitable Winegrowing, Australian Society of Viticulture and Oenology Mildura Seminar, Mildura, Victoria, Australia, 2-3 August 2017.

Skewes, M., Wang M., Whitty, M., Lam, S., Petrie, P., and Liu, S. (2017) Smart Phone Assessment of Water Stress, AWRI Webinar, 2 November 2017.

Posters

Skewes M, Liu S, Whitty MA, and Petrie P. (2016) Using a Smartphone to Measure Vine Water Status, Australian Wine Industry Technical Conference, Adelaide, Australia, July 2016.

Media

Johnson, R (2017) New App to Measure Water Stress in Grapevines, 24 January 2017. A series of radio interviews and syndicated articles were published as a result of this media release.

MEDIARELEASE

Tuesday 24 January 2017

Contact: Rob Johnson, SARDI Communications Adviser, 0423 292 867

Follow us on Twitter @SA_PIRSA

SOUTH AUSTRALIAN RESEARCH & DEVELOPMENT INSTITUTE
PIRSA

Wine Australia

New app to measure water stress of grapevines

A new smartphone app that helps grape growers measure the water status of their vines is being trialled across Australia.

The portable viticultural tool has the potential to help grape growers make improved water management decisions for their vineyards.

Grape growers use a thermal camera attached to their smartphone to take images of the canopy of the grapevine. The image is analysed by the app, which calculates the vine water status.

The technology is being tested by 15 vineyards in South Australia, Victoria, New South Wales and Tasmania for the rest of the growing season.

The Wine Australia-funded project is being led by the South Australian Research and Development Institute (SARDI), a division of Primary Industries and Regions SA (PIRSA), in close collaboration with The University of New South Wales (UNSW).

Quotes attributable to Dr Kathy Ophel-Keller, Acting Executive Director of the South Australian Research and Development Institute

Water and associated pumping costs can be a significant component of the production costs for grape growers.

Uncontrolled water stress has the potential to reduce the yield and quality of grapes and the resulting wine, which in turn reduces the return to growers.

The management of vine water status is a key tool for grape growers to regulate yield and optimise fruit quality and style.

This new app offers grape growers instant feedback on the water status of their vines, and provides them with the flexibility to assess multiple blocks or sections of blocks, and to make irrigation decisions in real time.

Quotes attributable to Dr Liz Waters, General Manager of Research, Development and Extension at Wine Australia

Irrigating effectively and efficiently helps to optimise vineyard production to produce high-quality winegrapes for fine Australian wines.

PREMIUM FOOD AND WINE FROM OUR CLEAN ENVIRONMENT

SOUTH AUSTRALIA

Government of South Australia
Primary Industries and Regions SA

SARDI
SOUTH AUSTRALIAN RESEARCH AND DEVELOPMENT INSTITUTE

Through many years of extensive research, methods have been developed to assess grapevine water status. This new app provides a portable solution to measure water status quickly and easily in the vineyard.

The app allows growers to make informed irrigation decisions that support the production of high-quality fruit grown to specification.

Background

The 18 month project aimed to evaluate a range of smart phone-based sensing systems to develop a cheap, easy-to-use vine water status monitoring app, to assist growers to manage irrigation.

Initial trial results found the thermal camera was the easiest to use and provided accurate information.

The app was developed by UNSW and the tool is now being tested by a variety of wineries, with their feedback helping to inform the further development of the innovative technology.

The aim is to release the final version of the app later in 2017.

Jayakody, H., Liu, S., Whitty, M., and Petrie, P. (2017) Microscope image based fully automated stomata detection and pore measurement method for grapevines. Plant Methods 13, 94.

Jayakody *et al. Plant Methods (2017) 13:94*
DOI 10.1186/s13007-017-0244-9

Plant Methods

RESEARCH

Open Access

Microscope image based fully automated stomata detection and pore measurement method for grapevines

Hiranya Jayakody[1*], Scarlett Liu[1], Mark Whitty[1] and Paul Petrie[2,3]

Abstract

Background: Stomatal behavior in grapevines has been identified as a good indicator of the water stress level and overall health of the plant. Microscope images are often used to analyze stomatal behavior in plants. However, most of the current approaches involve manual measurement of stomatal features. The main aim of this research is to develop a fully automated stomata detection and pore measurement method for grapevines, taking microscope images as the input. The proposed approach, which employs machine learning and image processing techniques, can outperform available manual and semi-automatic methods used to identify and estimate stomatal morphological features.

Results: First, a cascade object detection learning algorithm is developed to correctly identify multiple stomata in a large microscopic image. Once the regions of interest which contain stomata are identified and extracted, a combination of image processing techniques are applied to estimate the pore dimensions of the stomata. The stomata detection approach was compared with an existing fully automated template matching technique and a semi-automatic maximum stable extremal regions approach, with the proposed method clearly surpassing the performance of the existing techniques with a precision of 91.68% and an F1-score of 0.85. Next, the morphological features of the detected stomata were measured. Contrary to existing approaches, the proposed image segmentation and skeletonization method allows us to estimate the pore dimensions even in cases where the stomatal pore boundary is only partially visible in the microscope image. A test conducted using 1267 images of stomata showed that the segmentation and skeletonization approach was able to correctly identify the stoma opening 86.27% of the time. Further comparisons made with manually traced stoma openings indicated that the proposed method is able to estimate stomata morphological features with accuracies of 89.03% for area, 94.06% for major axis length, 93.31% for minor axis length and 99.43% for eccentricity.

Conclusions: The proposed fully automated solution for stomata detection and measurement is able to produce results far superior to existing automatic and semi-automatic methods. This method not only produces a low number of false positives in the stomata detection stage, it can also accurately estimate the pore dimensions of partially incomplete stomata images. In addition, it can process thousands of stomata in minutes, eliminating the need for researchers to manually measure stomata, thereby accelerating the process of analysing plant health.

Keywords: Stomatal morphology, Automatic stomata detection, Cascade object detection, Image processing, Skeletonization, Machine learning, Stomata, Grapevines

*Correspondence: hiranya.jayakody@unsw.edu.au
[1] School of Mechanical and Manufacturing Engineering, UNSW, Sydney, Australia
Full list of author information is available at the end of the article

Background

Microscopic study of leaf epidermises aid researchers to gain a better understanding on the overall behavior and health of plants [1]. A microscope image of a leaf epidermis can provide a clear view of guard cells, epidermal cells, stomata and plant leaf veins. Among these elements, stomata, surrounded by guard cells, play a major role in protecting the plant against water loss and regulating the gas exchange with the external environment [2, 3]. As a result, the behavior of stomata provides key information on the water stress level, food production rate and the overall health of the plant [1, 4–6]. In an agricultural scenario, analysing stomatal behavior can lead to better resource management and yields [7, 8].

However, examining stomatal behavior from a microscope image is not a straightforward task. Different plants have different leaf structures, and biologists with expert knowledge are required to correctly identify and measure stomatal morphology. Currently, the most common approach to achieve this goal involves manual measurement of stomata pore dimensions using softwares such as ImageJ® [9]. These type of tools require the user to manually mark the points of interest such as pore boundaries, stoma length and width so that the tool can produce the relevant measurement results. ImageJ® also provides additional plugins in order to make tasks such as stomata identification easier, but users still need to manually tune parameters for each image to achieve reasonable results [10–12]. Even with the aid of such tools, the process of manually measuring stomata morphology is both time consuming and cumbersome. Due to the time constraints imposed by manual measurements, biologists are forced to select only a few stomata for measurement from each captured microscope image, and build statistical relationships and models using fewer data-points [13]. However, more robust statistical models can be built if all available data are measured. The solution therefore, would be to develop a fast, fully automated method which can accurately measure stomatal morphological features without any human intervention.

Several studies can be found on automatic detection and measurement of stomatal morphology. One of the first studies to investigate the possibility of automatically measuring stomata pore features was conducted by Omasa and Onoe [14]. In this research, a Hanning filter alongside a series of morphological operations is utilized in measuring the pore opening of sunflower stomata. However, this approach does not focus on correctly identifying stomata from a large microscope image in the presence of other background elements such as veins and dust particles. Instead, this method requires the input to be an image containing a single stoma. The work presented by Karabourniotis et al. [15] applies UV radiation to leaves, which as a result causes guard cells to emit a blue florescence. The plant leaves are then captured using a fluorescent microscope and the resulting images are filtered and segmented to extract stomata and guard cells. Even though this method produces reliable results, it requires a relatively featureless background as well as methods of applying UV radiation to the leaf. In addition, the work presented by Sanyal et al. uses image processing techniques on microscope images to classify different tomato types based on stomata structure [16]. A watershed technique is employed to extract a single stoma from a nearly featureless background. However, the proposed method would not perform well in the presence of multiple stomata and a feature-rich background.

More sophisticated approaches which aim to extract and measure stomata from feature-rich backgrounds can be found in the researches conducted by Laga et al. [13] and Liu et al. [17]. The work presented by Laga et al. [13] follows a template matching approach to identify and measure the stomata pore opening of wheat plants. Wheat has a very consistent leaf epidermal structure with wheat stomata roughly aligned in the same direction, which makes it suitable candidate for template matching. However, for irregular leaf structures this method requires more templates, and has the tendency to produce false positive results especially when there are vein structures which look similar to stomata. Furthermore, the stoma pore detection approach used in this research assumes that both the stoma and the guard cell boundaries are clearly captured by the microscopic image. However, in a practical scenario, the images captured are not perfect, and contain plenty of partially captured stomata. More recent research conducted by Liu et al. [17] focuses on detecting and measuring grapevine stomata by utilizing maximum stable external regions (MSER). Although less time consuming than using the ImageJ® tool, this semi-automatic method still requires the users to interactively choose correct results from a given image and manually tune a set of parameters for each image. In addition, this approach always identifies stomata pore openings as symmetric ellipses, which is not the case in reality.

In this paper, we aim to develop a fully automated method to identify and measure stomata pore dimensions of grapevines, using microscope images. The images are prepared by applying a layer of resin and nail polish onto the leaf surface, and then carefully removing the nail polish layer which carries an imprint of the leaf epidermis. The final microscope image is generated by placing the nail polish impression on a microscope slide. The microscope images used for this research contain feature-rich backgrounds and the quality of the images captured vary depending on external conditions. Unlike previous work, where classical image processing techniques are used, the authors of this paper have opted to adopt a machine learning based cascade object detector to identify the stomata in a microscopic image. A similar cascade classifier has been previously applied to estimate the density of stomata in oak leaves [18]. However, compared to the work in [18] which uses Haar-like features for classification, the work presented in this paper utilizes HOG features to build the cascade object detector. Using a HOG descriptor, which is known to perform well in capturing the overall shape of an object, allowed the authors to build an accurate classifier using a less number of training samples (550 positive samples and 210 negative samples) compared to the work in [18] (10,000 positive samples and 3000 negative samples). It will be later shown that the training time required for a HOG based classifier is drastically lower compared to the Haar based COD proposed in [18] which took several days to train. A lower training time allows researchers to easily modify the proposed approach to train for different plant types with limited computing resources.

Once the stomata are automatically identified using the proposed COD algorithm, these regions of interest are cropped out and segmentation and skeletonization techniques are applied to the cropped image in order to measure the stoma pore boundary. Contrary to existing methods which require sharp, clean microscopic images for processing, the proposed approach, with the help of skeletonization, can estimate the stoma pore boundary under imperfect conditions where the stoma and guard cell boundaries are not fully visible, due to errors in applying resin, peeling off the nail polish layer etc. Here, skeletonization refers to the process of reducing a region to a skeletal remnant whilst preserving the connectivity features of the original image [19, 20]. The final result is a fully automated start-to-end stomata detection and measurement solution, where the input is a microscopic image of varying quality, and the output a set of stomatal morphologies.

The performance of this two stage method is then compared with the MSER method proposed by Liu et al. [17] and template matching method proposed by Laga et al. [13] using 50 microscopic images of cabernet sauvignon. Results show that the proposed approach is able to identify stomata more reliably, and produces accurate results in measuring the stomata pores.

The paper is organized as follows. In the "Methods" section, the image processing and machine learning techniques used to identify and measure stomatal properties are discussed in detail with examples. The experimental results of the study and comparisons with existing methods are presented in the "Results" section. The last section concludes the paper.

Methods

The main aim of this work is to develop a fully automated solution for stomata measurement, where a microscopic image is used as the input to the system and the corresponding morphological features of the stomata in the image are treated as the final output. The proposed methodology consists of two stages. The first stage aims at correctly identifying the stomata in a given microscopic image. Once, the stomata are automatically identified and cropped out from the original image, the second stage analyses and measures the morphological features of each individual stoma. The steps involved in both of these stages are discussed in detail from the next section onwards.

Cascade object detection algorithm to identify regions of interest

Cascade object detection (COD) algorithm is a multi-stage classification learner, where each stage is made up of a collection of weak learners. Each of these stages are trained using a technique called boosting. For the work presented in this paper, a COD which uses the Viola–Jones algorithm for face detection is re-trained for the purpose of identifying stomata [21, 22]. The COD approach inherently assumes that a large percentage of the image does not contain an object of interest. This in fact serves well for the question at hand, where the area covered by the stomata is small compared to the overall microscopic image area.

The COD approach is also known for reliably classifying objects of which the aspect ratio doesn't change drastically. Furthermore, this method is better suited for situations where there are no out of plane rotations of the object. Thus, COD can be identified as a good candidate for the stomata detection since all stomata lie on a 2D plane and have minor aspect ratio changes. Also note that the COD method employed for this task uses Histogram of Oriented Gradients (HOG) as the main learning descriptor [23]. The implementation procedure for the COD algorithm consists of two major steps.

1. Train the cascade object detection classifier using a set of positive images (images containing stoma) and a set of negative images (images of veins, dust particles and other features). The overall simplified operational procedure for an n stage cascade classifier is presented in Fig. 1. A detailed representation of the operations carried out by the initial stage and a general stage of the classifier are shown in Figs. 2 and 3 respectively.
2. Slide a window over the microscope image and use the trained COD classifier to check for a stoma inside the window. If a stoma is detected inside the sliding window, define that area as a region of interest (ROI).

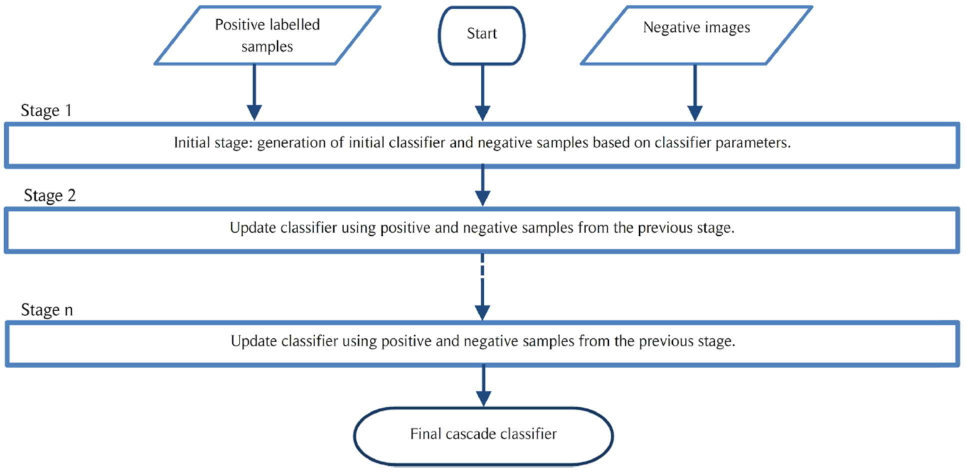

Fig. 1 The operational procedure of an n-stage cascade classifier

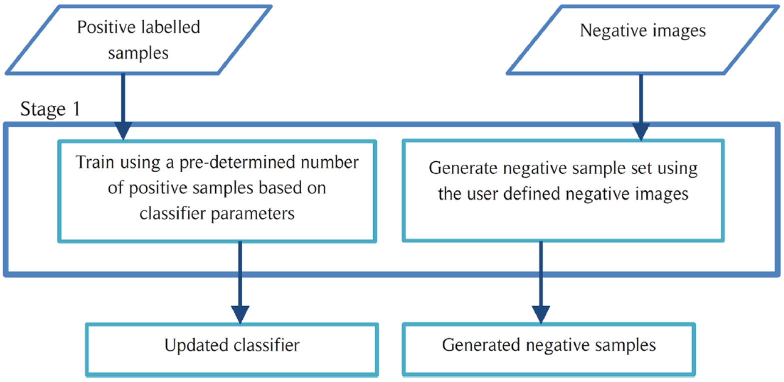

Fig. 2 Function of the initial stage of a cascade object detector

Figure 4 shows the COD classifier at work. The bounding boxes which contain stoma are cropped and then sent to the second stage where binary segmentation methods alongside skeletonization techniques are applied to measure the pore morphology.

Stomata pore measurement via binary image segmentation and skeletonization

Once the ROIs are identified and cropped, the next step is to detect and measure the stomatal pore in each ROI. Before proceeding with the pore measurements, it is important to observe the nature of the stoma captured. A closer look at the ROIs indicate that the stomata observed can be categorized into two types as,

1. Stomata with complete pore boundaries (see Fig. 5a.1).
2. Stomata with incomplete (discontinuous) pore boundaries (see Fig. 5b.1).

In order to develop reliable statistical models and relationships involving leaf epidermises, it is important

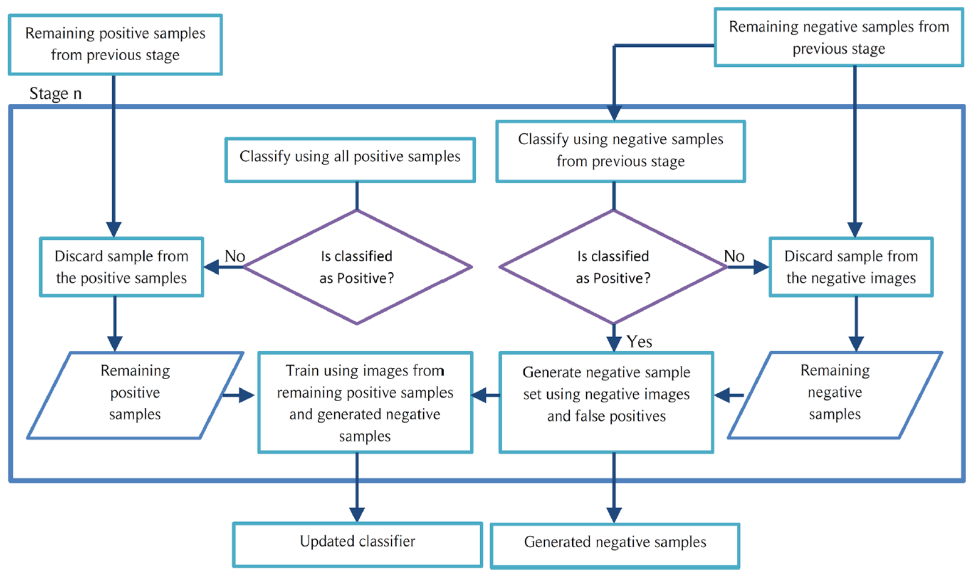

Fig. 3 Function of a general stage of a cascade object detector

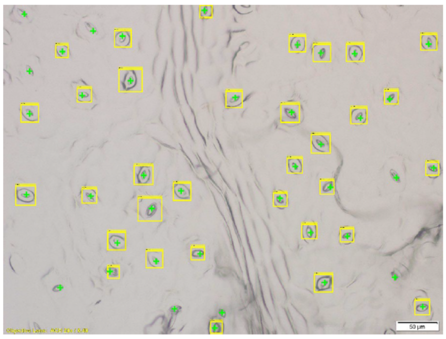

Fig. 4 A sample result of the COD based stomata detection method. The green crosshairs represent actual stomata. The yellow bounding boxes show automatically detected regions of interest (ROIs)

to collect as much data as possible from a given microscope image. To the best of our knowledge, all previous research inherently discard stomata with low quality and require sharp, clean, complete boundaries in order to derive pore measurements. In this work, a skeletonization based approach is proposed to overcome this issue and estimate pore boundaries for low quality stomata with discontinuous pore boundaries.

The stomatal pore measurement stage has two sub-stages:

1. Binary image segmentation: estimates pore measurements for high quality, complete stomata.
2. Skeletonization and ellipse fitting: estimates pore measurements for low quality incomplete stomata.

First, all cropped stomata images are fed through the binary image segmentation method. The binary image segmentation method can accurately estimate the stomatal pore areas for high quality images. However, this method fails when processing low quality images with discontinuous boundaries. Therefore, whenever this method fails in identifying the stomatal pore area, the corresponding low quality image is then fed into the skeletonization and ellipse fitting method. Adopting such a method ensures that pore boundaries are identified for the majority of the stomata detected under varying image quality.

Binary image segmentation

The following set of steps are employed to estimate the stoma morphology for complete pore boundaries.

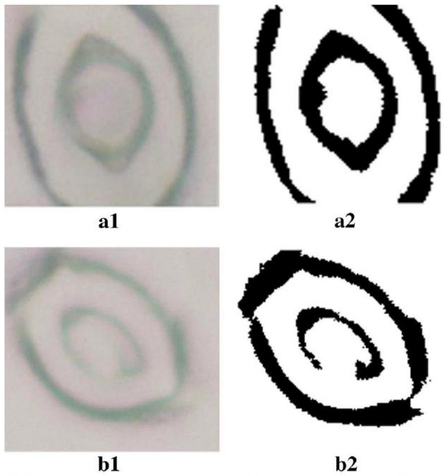

Fig. 5 Examples of stomata captured with varying quality. **a.1** Stoma with a complete pore boundary. **a.2** Binary segmentation result for a complete pore boundary. **b.1** Stoma with an incomplete pore boundary. **b.2** Binary segmentation result for an incomplete pore boundary

1. The image is sharpened, converted to grayscale and then converted to a binary image.
2. Independent regions (disconnected from each other) are identified on the binary image.
3. The region representing the stomatal pore opening is identified based on two assumptions: (a) the stoma is closer to the center of the ROI, (b) the pore area is smaller than a predefined upper limit. The upper limit of the pore area represents the approximate maximum area that can be covered by a stomatal pore. This parameter depends on the resolution and the zoom level of the microscopic image. The upper limit can be defined by briefly observing the original images and gaining an understanding on how large a typical stoma is (pixelwise).
4. The pore opening is marked and the morphological features such as area, major axis length, minor axis length and eccentricity are measured.

A visual representation of this method is shown in Fig. 6. This simple approach produces reliable results when the stoma is of good quality. However, if the stoma pore boundary is discontinuous, the binary image of the stoma would not contain a independent region which agrees with the two assumptions made in step 3 (see Fig. 5b.2 for such a condition). Therefore, such images are discarded and handed over to the skeletonization and ellipse fitting method. A detailed description of the skeletonization approach is presented in the next section.

Skeletonization and ellipse fitting

Image skeletonization refers to the process of reducing a selected region to a skeletal remnant which represents the medial axis of that region [19]. The following set of steps are applied to the images discarded by image segmentation sub-stage, with the aim of estimating stoma morphological features in the presence of discontinuous pore boundaries.

1. The image is sharpened, converted to grayscale and then converted to a binary image.
2. Independent regions (disconnected from each other) are identified on the binary image.
3. The binary image is inverted.
4. The independent regions on the image are skeletonized (also known as deriving medial axes). Each skeletal remnant would be a vector containing pixel coordinates.
5. The skeletal remnant associated with the pore boundary is then identified based on two assumptions: (a) the skeletal remnant associated with the stoma is

Fig. 6 The binary image segmentation process. **a** Original image. **b** Binary image. **c** Identify pore region. **d** Pore boundary overlaid on the original image

closer to the center of the ROI. (b) The length of the skeletal remnant lies between a pre-defined upper and lower limit.

6. Once the correct skeletal remnant is identified, generate an ellipse which fits the points of the skeletal remnant.
7. This ellipse is then used as a mask on the binary image derived in step 2. The independent region inside this mask is identified as the stoma pore.

A visual representation of this step-by-step approach is shown in Fig. 7. Skeletonization and ellipse fitting, together with binary image segmentation ensures that morphological features are measured for a large percentage of the initially detected ROIs. Compared to the traditional approach of manually measuring stomata which drastically limits the number of stomata which can be measured, this novel approach provides a comprehensive solution which provides pore measurements for a large number of stomata in quick time.

Results

The performance of the two stage stomata measurement method was compared with Liu's MSER approach and Laga's template matching approach. Programs for all three methods were developed using Matlab® R2017a.

Training procedure

The training step of COD was conducted using 550 positive samples where each image contained a single stoma, and 210 negative samples which contained other leaf epidermis features such as veins and dust particles. The classifier consists of 8 stages, and utilizes HOG features as the main descriptor. The visual representation of the HOG features on positive samples are shown in Fig. 8. The training process took approximately 7 min, inside the Matlab® environment on a 2.2 GHz Intel® Core i7-4702MQ CPU with 16 GB RAM. Note that COD training with HOG features takes drastically less processing time compared to the classifier used in [18] which took several days to train.

Data collection

The trained classifier was then tested on a separate 50 microscope images collected from cabernet sauvignon leaves containing 2012 stomata. The images were prepared using the conventional approach, where a layer of resin and nail polish are applied to the leaf epidermis, and an imprint of the leaf surface is captured by removing the nail polish layer and placing it on a microscope slide. The microscope images were captured using an Olympus® DP73 camera attached to an Olympus® BX53 microscope. The image resolution was set at 4800 × 3600 pixels, with a magnification of 8.6 pixels/μm.

Stomata detection

The stomata detection capability of the proposed COD approach was put to test first. In order to measure the performance improvements of the proposed method, two other existing methods, namely, Laga's template matching approach and Liu's maximum stable extremal region approach, were applied to the same 50 images. Since Liu's MSER approach is not a fully-automated method, we tuned the MSER parameters such that it provided best possible results for the given image set, and then automated the process in order to make the three methods more comparable. The template matching method was implemented using 20 stoma templates. Detailed implementation instructions for both template matching and MSER methods can be found in [13] and [17].

The corresponding results obtained after applying these three methods to 50 microscopic images are presented in Tables 1 and 2. The proposed method not only generated the highest number of true positives, it also resulted in the least number of false positives. Thus, the results clearly reflect the superiority of the the cascade classifier compared to the other two existing autonomous approaches. Further statistical analysis of the results showed that the proposed COD approach had the highest precision, recall and accuracy rates among the three methods (see Table 2). It is also the only method to surpass an F1-score of 0.80. The low number of false positive results generated by COD can be identified as the main reason contributing to this superior F1-score.

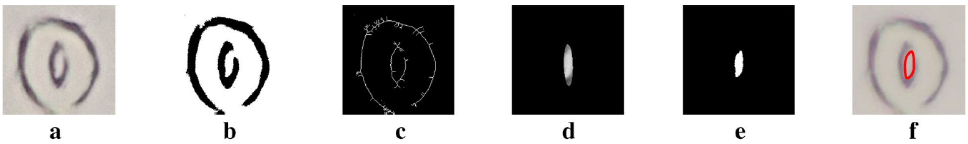

Fig. 7 Skeletonization and ellipse fitting process. **a** Original image. **b** Binary image. **c** Derivation of independent line segments via skeletonization. **d** Fit ellipse to the skeletal remnant representing the pore opening. **e** Binarize the region inside the ellipse and identify regions. **f** Pore boundary overlaid on the original image

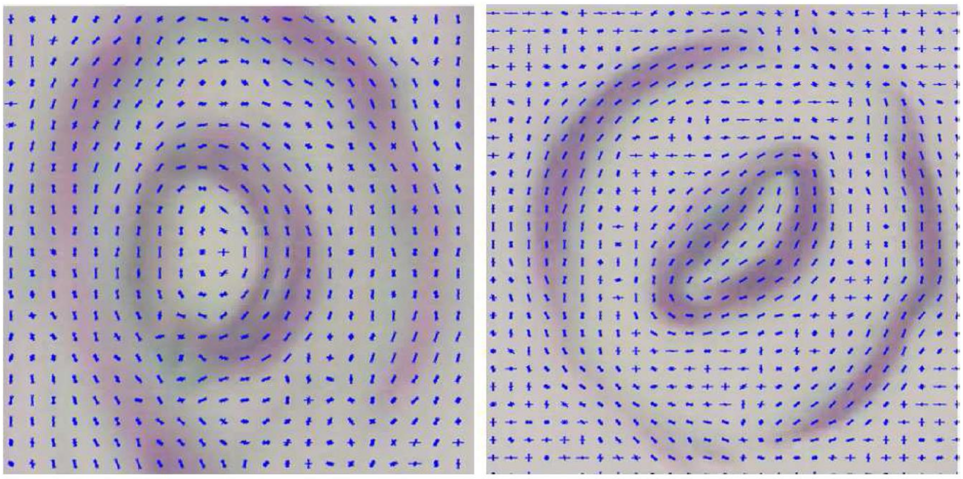

Fig. 8 HOG feature visualization for positive samples

Table 1 Numerical results obtained for template matching, MSER and COD methods, using 50 microscopic images containing 2012 stomata

	Actual number of stomata	ROIs detected	True positive	False positive	False negative
Template matching	2012	2331	1324	1007	688
MSER	2012	1398	746	652	1266
COD (proposed)	2012	*1742*	*1597*	*145*	*415*

The numbers for the proposed method were italisized to emphasize the improvement of the proposed approach

Table 2 Statistical results obtained for template matching, MSER and COD methods, using 50 microscopic images containing 2012 stomata

	Precision (%)	Recall (%)	Accuracy (%)	F1-score
Template matching	56.64	65.50	43.95	0.60
MSER	53.36	37.08	28.00	0.44
COD (proposed)	*91.68*	*79.37*	*74.04*	*0.85*

The numbers for the proposed method were italisized to emphasize the improvement of the proposed approach

Stomata measurements

The next step was to test the performance of the second stage of the proposed approach. In this stage, the main aim of the algorithm was to estimate the morphological features of the stomata pores. For this experiment, the 1742 ROIs detected through the COD method were used as the input. The corresponding results are presented in Table 3. Out of 1742 identified ROIs, the binary image segmentation method combined with skeletonization was able to generate results for 1267 stomata while discarding 475 ROIs. Further analysis showed that the 475 ROIs discarded by the pore estimation method included false positives generated by the COD as well as stomata of which the pore boundary could not be identified with any confidence, due to the image being out of focus or stoma being partially captured. Next, the generated 1267 estimations were visually inspected. These inspections showed that this approach was able to correctly identify the pore boundaries 86.27% of the time. The inaccurate results (174 out of 1267 ROIs) often identified the guard cell boundary as the stoma opening. However, this small number of inaccuracies does not pose a threat to the final result, as the user can easily visually inspect and remove such results from the dataset. It is important to note that the time spent on discarding inaccurate results via visual inspection is negligible compared to the time consumed in manually marking over a 1000 stoma pore openings.

Let us now consider the correctly marked stomata. It is important to measure how the automatically generated stomatal pore measurements compare with manually

Table 3 Results obtained for stomata pore estimations for 1742 ROIs

	Number of ROIs as input	Discarded ROIs	Accurate pore identifications	Inaccurate pore identifications	Identification accuracy
Binary image segmentation with skeletonization and ellipse fitting	*1742*	*475*	*1093*	*174*	86.27%

The numbers for the proposed method were italisized to emphasize the improvement of the proposed approach

marked stomatal pores traced using tools similar to ImageJ®. In order to make this comparison, the stoma boundary was manually marked under expert supervision for 70 randomly generated ROIs. These manually marked boundaries were considered as the ground truths. Then the manually measured parameters were compared with the measurements generated by the proposed automated method. The following equations were used to estimate the major axis length, a, and minor axis length, b,

$$a = \sqrt{\frac{A}{\pi\sqrt{1-E^2}}}, \tag{1}$$

$$b = \sqrt{\frac{A\sqrt{1-E^2}}{\pi}}, \tag{2}$$

where, A is the area of the stoma pore and E is the eccentricity of the detected pore. The corresponding results of the experiment are presented in Table 4. Here, the term accuracy is defined as,

$$\text{Accuracy (\%)} = |(Y - \hat{Y})/Y| \times 100, \tag{3}$$

where, Y is the actual value, and $\hat{Y}$ is the estimated value. According to the results, the pore area traced by the automated method is always slightly larger than the manually marked area but holds an accuracy reading of 89.03%. However, the eccentricity values are highly accurate as the errors in major and minor axis length measurements are quite uniform (i.e: similar estimation errors in a and b would not highly affect the term b/a). The average accuracies for both major axis length and minor axis length surpass 90%, with accuracy readings of 94.06 and 93.31% respectively. A side-by-side visual comparison between the ground truth and the estimation for 12 test images is presented in Fig. 9.

Table 4 Comparison of automatic stomatal pore measurements with manual measurements derived using ImageJ®

Number of stomata compared	Avg. area accuracy	Avg. eccentricity accuracy	Avg. major axis length accuracy	Avg. minor axis length accuracy
70	89.03%	99.43%	94.06%	93.31%

Observing the results, it can be concluded that the fully automated method is able to provide accurate morphological measurements for 1093 stomata out of 2012 available stomata in a small amount of time. Please note that the two stages together have discarded 890 stomata due to various reasons such as stoma being too blurry, not properly captured etc. The time consumed by an Intel i7 computer with 16 GB RAM to process the 50 images of high resolution (4800 × 3600 pixels) was measured to be 10 min (roughly 12 s to process 40 stomata). These results suggest that the proposed approach can save a huge amount of time in processing large sets of microscopic data, when compared to manual approaches.

Discussion

As per the results, the proposed two stage fully automated method is able to out-perform existing stomata detection method as well as accurately measure stoma pore dimensions. The reasons which result in such an improvement are discussed next.

Figure 10 shows the results generated by the three methods for a sample microscopic image. The template matching approach works well in highlighting areas containing stomata as shown in Fig. 10a. Note that this is the first time the template matching approach was applied to a leaf structure with stomata oriented in all directions. In this scenario, the template matching method is prone to highlighting other epidermal elements such as veins and dust particles which align well with some stomata and have similar thicknesses. This causes the template matching method to generate a high number of false positives. On the other hand, the MSER approach proposed by Liu et al. searches for stable elliptical regions in the image. Thus, their approach is not robust enough to differentiate between stoma pore openings, outer guard cell walls and veins containing elliptical patterns. This results in a high number of false positives as well. In addition, this method tends to discard stomata pores of which the interior is not stable enough for detection. These issues are clearly illustrated in Fig. 10b.

The proposed cascade object detection approach identifies stomata by learning their overall appearance. Thus, it is able to identify stomata in a more robust manner, whilst keeping the number of false positives to a

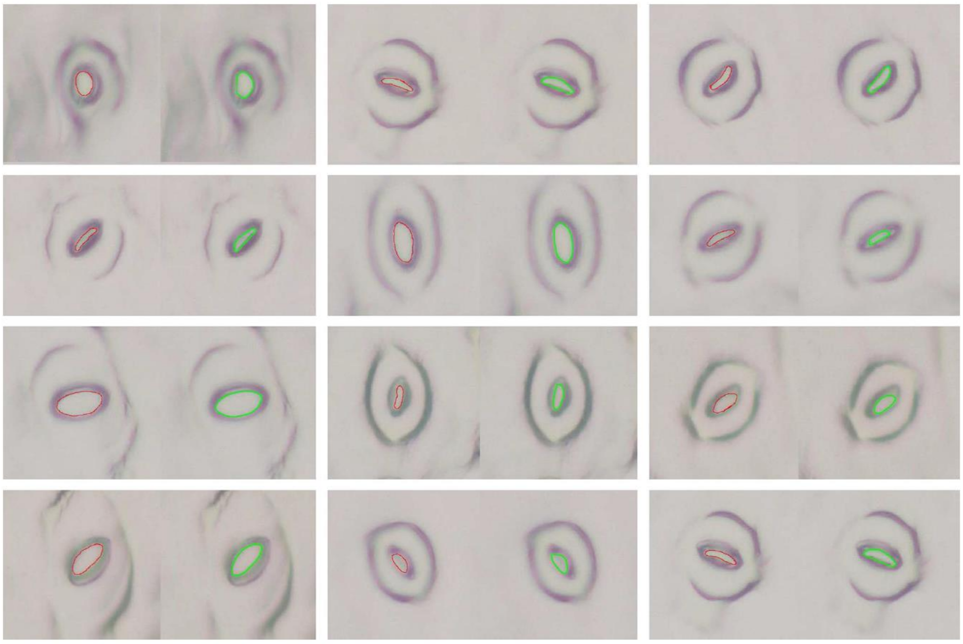

Fig. 9 A sample segment of stomata pore measurement results. A red trace represents a manually marked (ground-truth) stoma pore. A green trace represents automatically measured pore for the same stoma

minimum. However, this method too would ignore stomata which look considerably different from the training data set (e.g: blurred stomata, partially captured stomata). Furthermore, as a learning algorithm, the performance of the proposed cascade classifier is subject to change depending on the hyper-parameters (number of stages, number of false positives allowed per stage etc.) used during learning as well as the nature of the training dataset used. Special attention should be paid to the size and the features captured by the training datasets in order to produce the best possible results. This cascade classifier approach can successfully perform with a wide range of leaf types. However, the classifier would require re-training with suitable training data for leaf types with considerably different stomata or background structure.

Let us now consider the stomata pore measurement process. The proposed pore measurement methodology, which involves binary image segmentation combined with skeletonization and ellipse fitting, does not require stoma boundaries to be sharp and continuous like Laga's template matching approach. It is fully capable of estimating stoma pore dimensions even in cases where the pore boundary is only partially visible in the image. However, in order to estimate the pore dimensions for a partially complete boundary, the boundary should be at least 60–70% complete. In other words, the implemented ellipse detection algorithm struggles to derive a confident estimate for boundaries which are more than 50% incomplete. This is one main reason for the stomata pore measurement stage to discard 475 ROIs from the 1742 detected ROIs (see Table 3).

Conclusions

This paper presented a fully automated start-to-end solution for estimating stomatal morphological features of grape leaves. This two stage approach, which comprises of a cascade object detector to identify stomata in an image, and a combination of segmentation, skeletonization and ellipse fitting techniques to measure the stomata pore opening, was able to perform better than recently developed automated stomata detection methods. The COD approach identified stomata with a precision of 91.68% and an F1-score of 0.85. Out of the identified stomata, this approach managed to correctly trace the pore

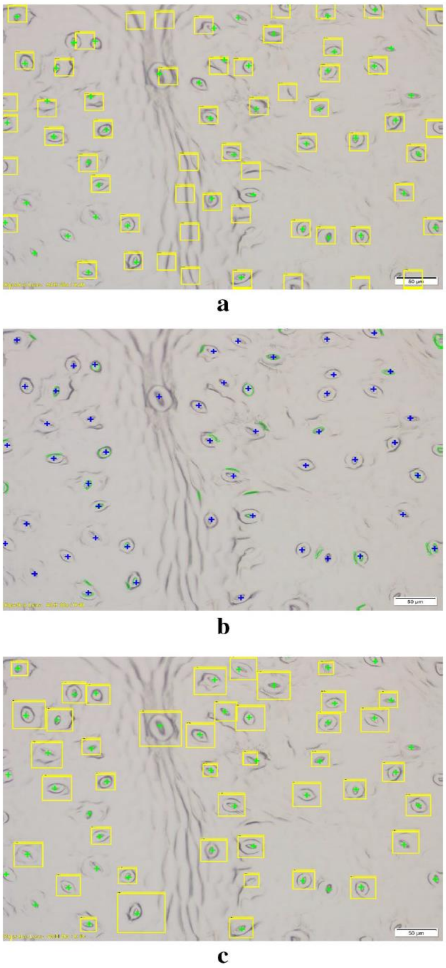

Fig. 10 Stomata identification results for three different methods. **a** Result for Laga's template matching method. **b** Result for Liu's MSER method. **c** Result for the proposed COD method

boundary of the stoma 86.27% of the time. Comparisons with ground truths show that the proposed approach measures the pore area with an accuracy of 89.03% the eccentricity with an accuracy of 99.43%. Compared to existing pore measurement methods, the proposed approach can estimate pore dimensions for stoma with incomplete pore boundaries. All the tests were conducted using grape leaves of type cabernet sauvignon. The authors intend to extend this research to test on different varieties of grapes and other plant types.

Abbreviations
COD: Cascade object detection; HOG: Histogram of oriented gradients; MSER: Maximally stable extremal regions; UV: Ultra violet.

Authors' contributions
HJ develop the cascade stomata detection algorithm and stomata pore measurement algorithm. Implement existing methods for comparison purposes. Conduct comparisons and derive results. Draft manuscript. SL conduct initial work on the MSER method. MW Project supervision and identifying main goals of the project. Contribution to writing the paper. PP preparing microscopic images for the research. Expert supervision in marking the groundtruths for the stomatal pore measurements. All authors read and approved the final manuscript.

Author details
[1] School of Mechanical and Manufacturing Engineering, UNSW, Sydney, Australia. [2] The Australian Wine Research Institute (AWRI), Adelaide, Australia. [3] South Australian Research and Development Institute (SARDI), Adelaide, Australia.

Acknowledgements
We would like to thank Wine Australia for funding the research, and South Australia Research and Development Institute (SARDI) and Australian Wine Research Institute (AWRI) for leading this research. Our acknowledgements also go to Mickey Wang for his assistance in collecting and capturing data from the field.

Competing interests
The authors declare that they have no competing interests.

Availability of data and materials
The datasets used and/or analysed during the current study are available from the corresponding author on reasonable request.

Consent for publication
Not applicable.

Ethics approval and consent to participate
Not applicable.

Funding
This project was funded by Wine Australia, under Project ID FPA001179: Smartphone based image analysis to assess vine water stress.

Publisher's Note
Springer Nature remains neutral with regard to jurisdictional claims in published maps and institutional affiliations.

Received: 21 July 2017 Accepted: 25 October 2017
Published online: 08 November 2017

References
1. Pillitteri LJ, Torii KU. Mechanism of stomatal development. Annu Rev Plant Biol. 2012;63:12–1124.
2. Osakabe Y, Osakabe K, Shinozaki K, Tran L-SP. Response of plants to water stress. Front Plant Sci. 2014;5(March):86.
3. Lawson T, Blatt MR. Stomatal size, speed, and responsiveness impact on photosynthesis and water use efficiency. Plant Physiol. 2014;164(4):1556–70.
4. Wolf A, Anderegg WRL, Pacala SW. Optimal stomatal behavior with competition for water and risk of hydraulic impairment. Proc Natl Acad Sci. 2016;113(46):7222–30.

5. Lawlor DW. Limitation to photosynthesis in water-stressed leaves: stomata vs. metabolism and the role of ATP. Ann Bot. 2002;89:871–85.
6. Chaves MM, Pereira JS, Maroco J, Rodrigues ML, Ricardo CPP, Osorio ML, Carvalho I, Faria T, Pinheiro C. How plants cope with water stress in the field? Photosynthesis and growth. Ann Bot. 2002;89(SPEC. ISS.):907–16.
7. Hopper DW, Ghan R, Cramer GR. A rapid dehydration leaf assay reveals stomatal response differences in grapevine genotypes. Hortic Res. 2014;1(October 2013):2.
8. Giorio P, Sorrentino G, D'Andria R. Stomatal behaviour, leaf water status and photosynthetic response in field-grown olive trees under water deficit. Environ Exp Bot. 1999;42(2):95–104.
9. ImageJ: image processing tool (1997–2017). National Institute of Health
10. Maloof JN, Nozue K, Mumbach MR, Palmer CM. LeafJ: an ImageJ plugin for semi-automated leaf shape measurement. J Vis Exp. 2013;71:2–7.
11. Cheng Y, Cao L, Wang S, Li Y, Wang H, Zhou Y. Analyses of plant leaf cell size, density and number, as well as trichome number using cell counter plugin. Bio-protocol. 2014;4(13). doi:10.21769/BioProtoc.1165.
12. Schneider CA, Rasband WS, Eliceiri KW. NIH image to ImageJ: 25 years of image analysis. Nat Methods. 2012;9:671–5.
13. Laga H, Shahinnia F, Fleury D. Image-based plant stomata phenotyping. In: International conference on control. Singapore: Automation, Robotics and Vision, Marina Bay Sands; 2014. p. 217–22.
14. Omasa K, Onoe M. Measurement of stomatal aperture by digital image processing. Plant Cell Physiol. 1985;25(8):1379–88.
15. Karabourniotis G. Epicuticular phenolics over guard cells: exploitation for in situ stomatal counting by fluorescence microscopy and combined image analysis. Ann Bot. 2001;87(5):631–9.
16. Sanyal P, Bhattacharya U, Bandyopadhyay SK. Analysis of SEM images of stomata of different tomato cultivars based on morphological features. In: Proceedings—2nd Asia international conference on modelling and simulation, AMS 2008; 2008. p. 890–4.
17. Liu S, Tang J, Petrie P, Whitty M. A fast method to measure stomatal aperture by MSER on smart mobile phone. In: Imaging and applied optics congress; 2016. p. 3–5.
18. Vialet-Chabrand S, Brendel O. Automatic measurement of stomatal density from microphotographs. Trees Struct Funct. 2014;28(6):1859–65.
19. Blum H. A transformation for extracting new descriptors of shape. In: Wathen-Dunn W, editor. Models for the perception of speech and visual form. Cambridge: MIT Press; 1967. p. 362–80.
20. Dyer CR, Rosenfeld A. Thinning algorithms for gray-sclae pictures. IEEE Trans Pattern Anal Mach Intell. 1979;1:1859–65.
21. Viola P, Jones M. Rapid object detection using a boosted cascade of simple features. In: Proceedings of the 2001 IEEE computer society conference on computer vision and pattern recognition. CVPR 2001, vol. 1; 2001. p. 511–8.
22. Viola P, Jones MJ. Robust real-time face detection. Int J Comput Vision. 2004;57(2):137–54.
23. Dalal N, Triggs B. Histograms of oriented gradients for human detection. In: 2005 IEEE computer society conference on computer vision and pattern recognition (CVPR'05), vol. 1; 2005. p. 886–93.

Appendix 2: Intellectual Property:

Identify the intellectual property and/or valuable information arising from the research.

The Vine Water Stress App is potentially valuable as an easy, quick and portable method to assess vine water status using a thermal camera. However, it is an application of techniques (both the Crop Water Stress Index and the image processing methods) that are available in the public domain.

Appendix 3: References

Anon (2015a) Compact - Seek Thermal. (Seek Thermal: Santa Barbara, California, USA).

Anon (2015b) FLIR one for Android / iOS. (FLIR Systems Inc: Wilsonville, Oregon, USA).

Brown, H.T. and Escombe, F. (1905) Researches on some of the physiological processes of green leaves, with special reference to the interchange of energy between the leaf and its surroundings. Proceedings of the Royal Society of London. Series B **76**, 29-111.

Charlesworth, P. (2005) Soil water monitoring. (Land & Water Australia: Braddon, ACT, Australia).

Choné, X., Leeuwen, C.V., Dubourdieu, D., Gaudillère, J.-P., van Leeuwen, C., Dubourdieu, D., and Gaudillère, J.-P. (2001) Stem Water Potential is a Sensitive Indicator of Grapevine Water Status. Annals of botany **87**, 477-483.

Costa, J.M., Grant, O.M., and Chaves, M.M. (2013) Thermography to explore plant-environment interactions. Journal of Experimental Botany **64**, 3937-3949.

Cozzolino, D., Fassio, a., Fernández, E., Restaino, E., and La Manna, a. (2006) Measurement of chemical composition in wet whole maize silage by visible and near infrared reflectance spectroscopy. Animal Feed Science and Technology **129**, 329-336.

De Bei, R., Cozzolino, D., Sullivan, W., Cynkar, W., Fuentes, S., Dambergs, R., Pech, J., and Tyerman, S. (2011) Non-destructive measurement of grapevine water potential using near infrared spectroscopy. Australian Journal of Grape and Wine Research **17**, 62-71.

Düring, H. and Stoll, M. (1996) Stomatal patchiness of grapevine leaves. 1. Estimation of non-uniform stomatal apertures by a new infiltration technique. Vitis **35**, 65.

Fereres, E. and Evans, R.G. (2006) Irrigation of fruit trees and vines: an introduction. Irrigation Science **24**, 55-57.

Fuentes, S., de Bei, R., Pech, J., and Tyerman, S. (2012) Computational water stress indices obtained from thermal image analysis of grapevine canopies. Irrigation Science **30**, 523-536.

Gerten, D., Heinke, J., Hoff, H., Biemans, H., Fader, M., and Waha, K. (2011) Global water availability and requirements for future food production. Journal of Hydrometeorology **12**, 885-899.

Gitz, D.C. and Baker, J.T. (2009) Methods for Creating Stomatal Impressions Directly onto Archivable Slides. Agronomy Journal **101**, 232.

Green, J. and Griffante, D. (2009) Australian Wine Industry Stewardship 2009 National Report. (Winemakers' Federation of Australia: Kent Town, Adelaide).

Guilioni, L., Jones, H.G., Leinonen, I., and Lhomme, J.P. (2008) On the relationships between stomatal resistance and leaf temperatures in thermography. Agricultural and Forest Meteorology **148**, 1908-1912.

Idso, S.B. (1982) Non-water-stressed baselines: A key to measuring and interpreting plant water stress. Agricultural Meteorology **27**, 59-70.

Jayakody, H., Liu, S., Whitty, M., and Petrie, P. (2017) Microscope image based fully automated stomata detection and pore measurement method for grapevines. Plant Methods **13**, 94.

Jones, H.G. (1999) Use of infrared thermometry for estimation of stomatal conductance as a possible aid to irrigation scheduling. Agricultural and Forest Meteorology **95**, 139-149.

Jones, H.G. (2004) Irrigation scheduling: Advantages and pitfalls of plant-based methods. Journal of Experimental Botany **55**, 2427-2436.

Jones, H.G., Stoll, M., Santos, T., de Sousa, C., Chaves, M.M., and Grant, O.M. (2002) Use of infrared thermography for monitoring stomatal closure in the field: application to grapevine. Journal of Experimental Botany **53**, 2249-2260.

Kappen, L., Schultz, G., and Vanselow, R. (1995) Direct observations of stomatal movements. In: Ecophysiology of Photosynthesis, Eds. E.D. Schulze and Caldwell, M.M. (Springer: Berlin, Germany) pp. 231-246.

Lawson, T., James, W., and Weyers, J. (1998) A surrogate measure of stomatal aperture. Journal of Experimental Botany **49**, 1397-1403.

Leinonen, I., Grant, O.M., Tagliavia, C.P.P., Chaves, M.M., and Jones, H.G. (2006) Estimating stomatal conductance with thermal imagery. Plant, Cell and Environment **29**, 1508-1518.

Maes, W.H., Baert, A., Huete, A.R., Minchin, P.E.H., Snelgar, W.P., and Steppe, K. (2016) A new wet reference target method for continuous infrared thermography of vegetations. Agricultural and Forest Meteorology **226–227**, 119-131.

Meister, M.H. and Nordenkampf, H. (2001) Stomatal imprints: A new and quick method to count stomata and epidermal cells. In: Handbook of Plant Ecophysiology Techniques, Ed. M.J.R. Roger (Kluwer: Amsterdam) pp. 235-250.

Mizuno, S., Noda, K., Ezaki, N., Takizawa, H., and Yamamoto, S. (2007) Detection of wilt by analyzing color and stereo vision data of plant. In: Computer Vision/Computer Graphics Collaboration Techniques, Eds. A. Gagalowicz and Philips, W. (Springer: Berlin, Germany) pp. 400-411.

Naor, A. (2006) Irrigation scheduling and evaluation of tree water status in deciduous orchards. Horticultural Reviews **32**, 111-165.

Ozdalga, E., Ozdalga, A., and Ahuja, N. (2012) The smartphone in medicine: a review of current and potential use among physicians and students. Journal of Medical Internet Research **14**, e128.

Peñuelas, J., Filella, I., Biel, C., Serrano, L., and SavÉ, R. (1993) The reflectance at the 950–970 nm region as an indicator of plant water status. International Journal of Remote Sensing **14**, 1887-1905.

Sadras, V.O., Montoro, A., Moran, M.A., and Aphalo, P.J. (2012) Elevated temperature altered the reaction norms of stomatal conductance in field-grown grapevine. Agricultural and Forest Meteorology **165**, 35-42.

Scholander, P., Hammel, H., Hemmingsen, E., and Bradstreet, E. (1964) Hydrostatic pressure and osmotic potential in leaves of mangroves and some other plants. Proceedings of the National Academy of Sciences **52**, 119-125.

Smart, R.E. (1974) Aspects of water relations of the grapevine (Vitis vinifera). American Journal of Enology and Viticulture **25**, 84-91.

Tanner, C.B. (1963) Plant Temperatures. Agronomy Journal **55**, 210-211.

Viola, P. and Jones, M.J. (2004) Robust real-time face detection. International Journal of Computer Vision **57**, 137-154.

White, S.C. and Raine, S.R. (2008) A grower guide to plant based sensing for irrigation scheduling. (National Centre for Engineering in Agriculture, University of Southern Queensland: Toowoomba, Queensland, Australia).

Zhang, Y., Teng, P., Shimizu, Y., Hosoi, F., and Omasa, K. (2016) Estimating 3D leaf and stem shape of nursery paprika plants by a novel multi-camera photography system. Sensors **16**, 874.

Appendix 4: Staff

Paul R. Petrie[a], Mickey Wang[b], Scarlett Liu[c], Stanley Lam[c], Hiranya Jayakody[c], Mark A. Whitty[c] and Mark A. Skewes[b]

[a]South Australian Research and Development Institute and the Australian Wine Research Institute
Glen Osmond, SA, Australia

[b]South Australian Research and Development Institute
Loxton Research Centre
Loxton, SA, Australia

[c]School of Mechanical and Manufacturing Engineering
University of New South Wales
Sydney, NSW, Australia

Appendix 5: Additional material

Instructions for Smartphone Application

The instructions provided to the beta testers for the use of the vine water stress app, as provided in January 2017.

Using Vine Water Stress App to measure Crop Water Stress Index of grapevines

Mark Skewes, Mickey Wang, Stanley Lam, Paul Petrie, Mark Whitty

Wine Australia

SARDI Government of South Australia

UNSW AUSTRALIA

Feedback

Our purpose in making this app available at this stage is to test it and fix any issues. To assist us in this process we ask you to provide as much feedback as you can.

In the first case please call or email Mickey Wang, the Technical officer for the project:

- 0472 841 884

mickey.wang@sa.gov.au

What's in the Box?

1. Oppo F1s mobile phone (not including SIM card) with the VWS App pre-installed.
2. FLIR One Thermal camera including charging cable.
3. Wet and dry reference leaves (red toweling mounted in an embroidery ring, wet reference is attached to a bottle to hold water for maintaining leaf wetness).

Note that the mobile phone does not contain a SIM card, at the first opportunity please connect it to a Wi-Fi network so the phone will check for updates to the app.

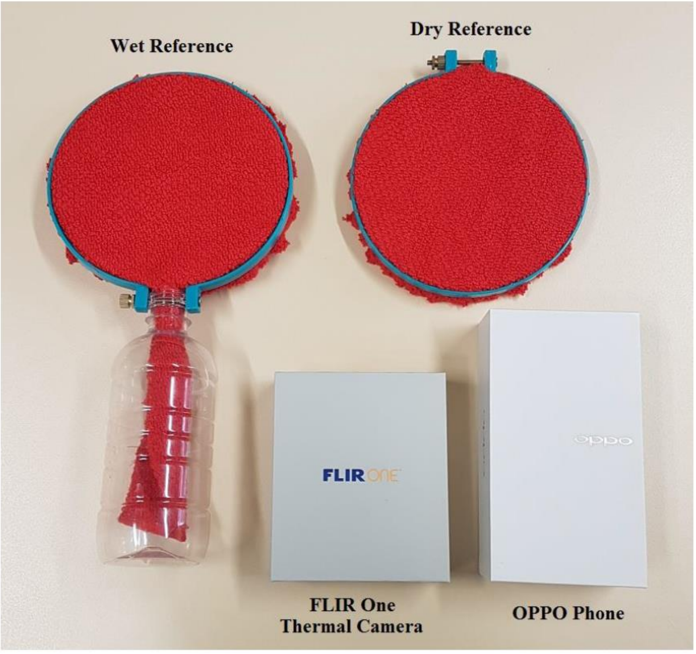

Figure 1 Contents of the box

Preparing to take the image

1. Ensure that both the Oppo phone and FLIR One camera are fully charged (or keep them on the charger in your vehicle).
2. Fill the wet reference bottle with water and wet the red toweling, ensure the wick is wet and reaches into the water (you may leave the bottle full all the time if you can store it upright, and just top up as needed).
3. Always avoid any kind of moisture source touching the dry reference. (E.g. don't carry the wet reference and dry reference in one hand. Don't touch the dry reference with wet hand.) If the dry reference is wet, don't use it until it has totally dried.
4. Select the vine that you are going to measure, hang the wet and dry reference leaves on the shaded side of the canopy and ensure that they are fully shaded (see Figure 2 for a suggestion of how to mount the reference leaves in the canopy, please feel free to create your own system to suit your canopy architecture).

Figure 2 Suggestion for mounting the reference leaves in the canopy

5. Leave the bottle and reference leaves in the field environment for a few minutes before taking the image so they can equilibrate with the vineyard temperature.

Taking the image

1. Activate the cell phone, plug in the FLIR One thermal camera and turn the FLIR One on using the button on the side. The VWS app will automatic run when it detects the FLIR One.
2. If the phone doesn't recognize the camera, turn the phone off and back on again, and try again.
3. The image will appear in RGB (normal colour) on the phone screen to aid with framing the photo.

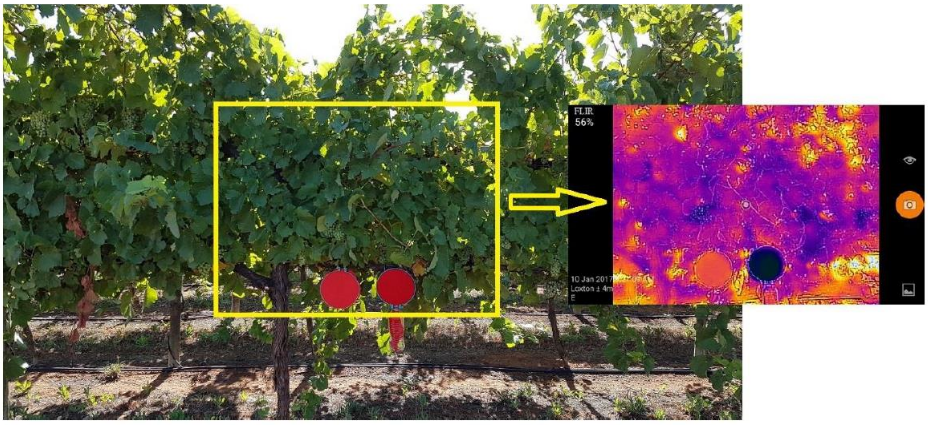

Figure 3 Yellow box indicates the recommended framing of the image for best results

4. Take the image from a distance of between 1 and 1.5 meters from the shaded side of the canopy, making sure both the wet and dry reference leaves are fully shaded and are included in the image (see Figure 3 for recommended framing of the image).
5. Press the 'button' on the app to take the image. A thermal image will now be shown on the phone.
6. The app will automatically select the wet and dry leaves (based on their colour and temperature) and highlight these with arrows. All other parts of the photo that aren't the grapevine canopy should be excluded from the analysis (denoted as RGB (normal colour) (Figure 4).
7. In the unlikely event that the wet or dry reference leaves haven't been selected correctly, move the blue (wet) or red (dry) arrow to the wet or dry reference leaf respectively.

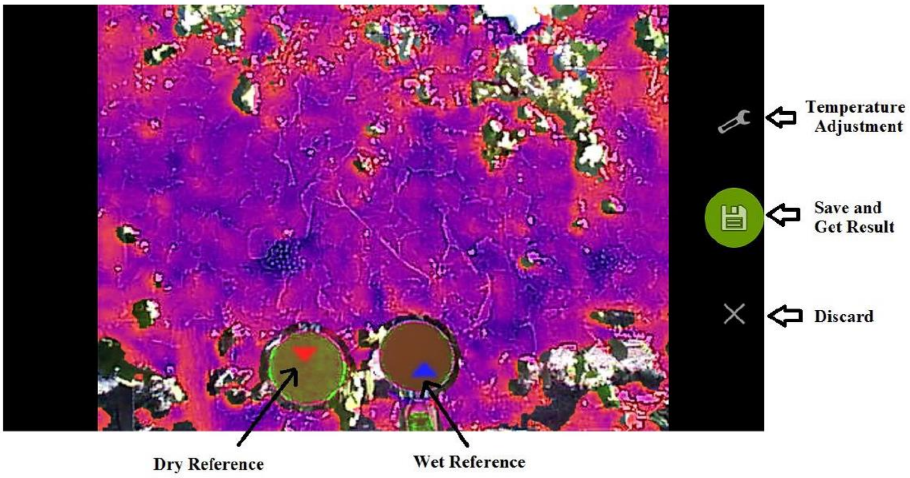

Figure 4 Initial thermal image screen

8. If a portion of the canopy is missing (can be seen as a RGB as opposed to a thermal view) from the image, or non-canopy components (e.g. a post or the ground) are included, select the tool symbol and adjust the two sliders at the bottom of the image until only the shaded part of the canopy is highlighted (Figure 5).

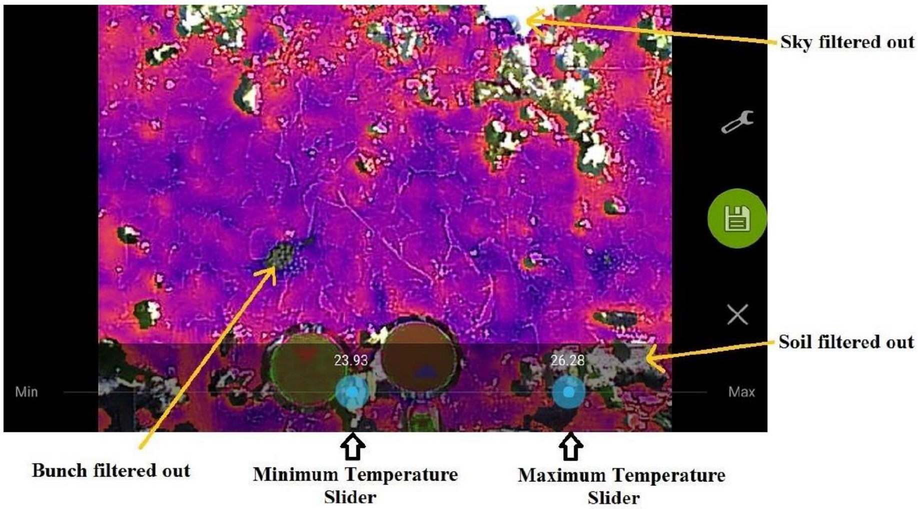

Figure 5 Temperature range adjustment tool

9. Press the 'save' icon, and a dialogue box will open which summarises the CWSI data for the image, and asks you to enter a block name. Press the blank space to call up the keypad, and enter an appropriate name. Press 'Done' and then 'OK' to save the image and data (Figure 6).

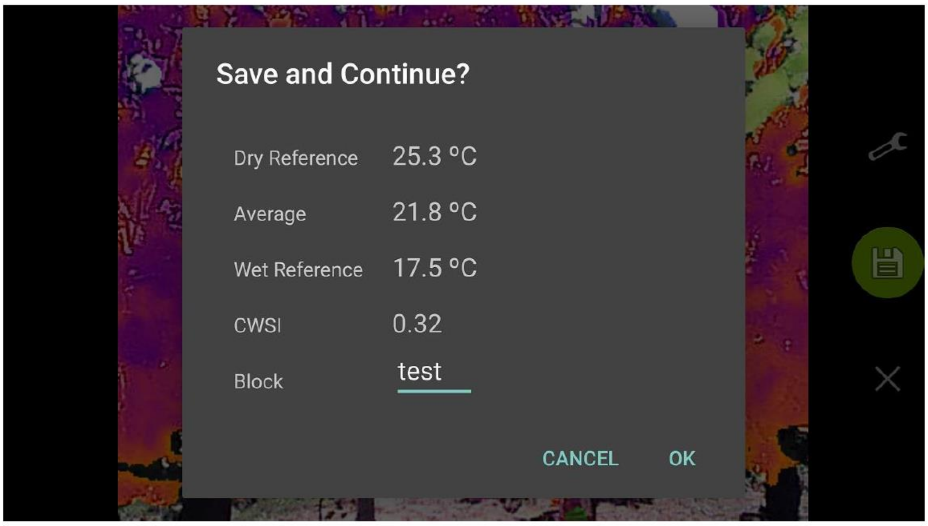

Figure 6 "Save" dialog box

10. It is recommended that you collect multiple images at each site to ensure that results are consistent, rapid changes in environment (especially cloud cover or wind) will influence the results.
11. When you return within range of a Wi-Fi network any images you have taken will also be uploaded to a database as soon as the phone is turned on and Wi-Fi connected. This will allow us to check the operation of the app and help troubleshooting any problems you may have. The FLIR One does not need to be connected or the app to be open for this to occur.

Interpreting Results

- Crop Water Stress Index (CWSI) result is a number between 0 and 1. Well irrigated vine should have a lower CWSI, while a water stressed vine will have a higher CWSI result.
- CWSI is usually lower in the morning, and increases gradually as the day becomes warmer. It will reach the highest level at approximately 3pm (or the hottest part of the day).
- The environment will also impact on CWSI. Just as you feel hotter when you stand in the sun, the CWSI would be higher on a sunny day compared to an overcast day.
- Appropriate benchmarks are still being developed for CWSI of a shaded canopy. For example, we need to confirm the impact of variety, canopy size and training system, phenology, and the time of day when the image is taken on CWSI.
- **Guidelines to CWSI (recorded on a shaded canopy):**
    1. **Above 0.7** on a sunny warm day represents some water stress.
    2. **Above 0.9** on a sunny warm day represents severe water stress.
    3. **Between 0.5 and 0.7** is in the normal range.
    4. **Readings below 0.5** are uncommon and would be expected to occur on a cool day with well irrigated vines.
- Until these benchmarks are better established the CWSI needs to be considered in an integrated manner with other methods of assessing vine water status, e.g. soil moisture and the condition of the canopy.
- If CWSI doesn't match the soil moisture results, e.g. CWSI shows a high result (stressed) but soil moisture sensor reports the soil as being wet, there could be an issue related to salinity or root damage.

Crop Water Stress Index – Background and Overview

<u>Traditional measurement of vine water status.</u>

There are a wide range of methods that have been used to assess vineyard water status and to make better irrigation scheduling decisions. Traditionally the Australian industry has relied on soil moisture monitoring as it can give a direct measure of soil content and its relatively slow changes in response to rainfall, irrigation and water use by the vines. Soil moisture sensors have been developed to be robust and are readily automated. Plant based methods of assessing water status in contrast are often far more dynamic in response to the environment. They integrate the amount of moisture available in the soil with the environmental conditions to indicate how stressed the vine is 'feeling'. Sudden changes in the environment such as an increase in wind or cloud cover can rapidly impact on these results.

<u>What is the Crop Water Stress Index?</u>

Plants' canopies are cooled due to the evaporation of water (transpiration) from leaves (like an evaporative air conditioner). When there is plenty of water available plants open their stomata (the pores on the leaves which regulate photosynthesis and transpiration), and the resultant evaporation of water from the leaf creates a cooling effect. Under drought conditions the stomata close to help conserve water and the temperature of the canopy increases as the rate of evaporative cooling drops. How open the stomata are (called the stomatal conductance) can be measured directly using a device called a porometer, or indirectly from the reduction in canopy temperature due to the evaporation. These measurements are an indication of the plant water status.

The Crop Water Stress Index (CWSI) provides an estimate of how cool the canopy is relative to the canopy of a crop that is well irrigated. A well irrigated crop that is transpiring as fast as possible is given a value of zero (in reality we rarely record values below 0.5), while a crop that is experiencing significant water stress would have a value of one. As it isn't practical to maintain well-watered and water stressed plants as references, wet and dry reference leaves are used as substitutes. The wet reference leaf represents the canopy of a fully irrigated plant, and the dry reference leaf represents the canopy of a badly water stressed plant.

The formula for the CWSI:

CWSI = (Canopy temperature – Wet reference temperature) / (Dry reference temperature - Wet reference temperature)

A thermal camera is a good tool to measure plant water status using the CWSI as it can easily assess the temperature of sections of the canopy as well as wet and dry references.

<u>How does CWSI relate to my vineyard?</u>

The CWSI is a direct measurement of the vine's water status. This is a benefit as you can assess how the vine is 'feeling', based on the weather conditions as well as how much moisture is in the soil. It can also be a drawback as transient changes in conditions, such as scattered cloud, can influence the results; potentially increasing the variation between measurements. These factors must be kept in mind when collecting and interpreting CWSI measurements.

The vine's water stress normally increases during the day. This is due to increasing temperature, normally until approximately 3pm, and the consumption of any water that was drawn from the profile and stored in the vine overnight. With other plant based measurements of water status (such as water potential), a consistent time of day (normally around mid-day) is selected to standardize the measurements. Targeting around mid-day (between 11am and 3pm) is also likely to give the most consistent results with CWSI.

Our testing of CWSI has focused on placing the reference leaves in the shade and assessing the shaded side of the canopy. In part this is to minimize variation in CWSI due to short term variation in cloud cover; however, all other things being equal you would expect to record a lower CWSI on a cloudy day then a sunny day.

<u>How could I use CWSI in my vineyard?</u>

There are a range of scenarios where CWSI could be used help inform irrigation scheduling that could complement or replace existing soil moisture monitoring systems.

Benchmark CWSI values are still being developed for grapevines based on shaded canopies. In our trials CWSI values below 0.5 have been rarely recorded and would represent very well-watered vines and cooler conditions on the day of measurement. Readings between 0.5 and 0.7 represent mid-range values. These can still occur on well-watered vines under hot conditions. For CWSI values above 0.7, some water stress is occurring and at above 0.9 this stress is severe. Regular assessment of the CWSI for your vineyard will help you develop an understanding of what values to expect from different blocks or varieties. Try and take measurements regularly to coincide with when you make your irrigation decisions.

If your target is to maximize vineyard yield then you would normally look to avoid any vine water stress, while not applying excessive water. Checking the CWSI immediately prior to applying irrigation would confirm that no stress has occurred. Preliminary estimates suggest that a CWSI of less than 0.7 recorded from a shaded canopy on a hot day, or 0.5 on a cooler day would suggest that your vines are being well irrigated.

If your target is to optimize quality and minimize water use as part of a regulated deficit irrigation strategy, then the CWSI could also be used to inform your irrigation decisions. If the vines are being maintained at a moderate water deficit (for example during the post flowering period) then irrigation could be withheld if the CWSI is below approximately 0.8 assuming very hot weather isn't forecast. Tracking the CWSI over time may give a viticulturist more confidence to extend the period between irrigation applications.

Soil moisture monitoring systems are normally point based at a limited number of sites across a vineyard, and it is uncommon for all the blocks within a vineyard to be covered. The thermal camera is very portable and can be used to compare different parts of a block and across blocks. If you are concerned that one section of a block may not be getting enough water then this provides an easy opportunity to check, or compare it to the section adjacent to the soil moisture probe.

Results of Beta Testers Survey

Results of the survey of the beta testers of the application completed from the end of vintage 2017.

Q1. The App was simple to use

	Strongly Disagree	Disagree	Neutral	Agree	Strongly Agree
No. of people selected				12	4
Percentage of people selected	0 %	0 %	0 %	75 %	25 %

Comment summary:
- It's a good concept to link the management method to a smartphone. It's great.
- The only negatives were: 1 the image editing tool. 2 the cumbersome nature of the reference paddles.
- Some difficulty in reading with the grass in the background.
- Can only take readings in the early morning or late evening because of row orientation.
- The App was user friendly and found the majority of the time worked well. Feedback from other users at our site found the app was also easy to operate on the phone.
- Easy to follow step by step.
- The app was simple to use once played or used it, not clear at first.

Q2. The methodology for using the app is clearly defined in the instructions

	Strongly Disagree	Disagree	Neutral	Agree	Strongly Agree
No. of people selected	1		2	9	4
Percentage of people selected	6.25 %	0 %	12.5 %	56.25 %	25 %

Comment summary:
- Confused by choosing the shady part of canopy for measurement.
- More direction on where to place the reference leaves would be good.
- The editing tool (temperature adjustment bar) and how this works / alters your results was not clearly spelt out.
- Very clear
- As far as I know the current version did not have a section with instructions. The printed instructions were easy to follow.
- Yes instructions detailed and pictures helped
- Yes. Clear instructions.
- The instructions were easy to read and understand.
- Well explained and easy to follow
- Instructions were OK but always found a question of 'how to do that'

Q3. I was comfortable installing the reference leaves for each set of measurements

	Strongly Disagree	Disagree	Neutral	Agree	Strongly Agree
No. of people selected	2	1	4	8	1
Percentage of people selected	12.5 %	6.25 %	25 %	50 %	6.25 %

Comment summary:

- Time consuming
- It's a two person job
- Feels awkward to carry and install
- Cumbersome if doing multiple sites.
- Dry references is very sensitive – the slightest amount of moisture can affect
- First time is a bit hard, once you work out the best way to place them this was not a concern.
- Some difficulty in getting the references to sit upright and stay in the canopy
- They should be smaller and attached to each other
- Suggest creating a framework to hold both references, would make it easier and prevent the paddles twisting
- It needed a bit of practice with sprawling canopy or traditional bush vine. Super easy on VSP and Scott Henry trellis.
- I was comfortable with installing the references but sometimes the canopy got in the way of the references
- Hard to attach to the large canopy with drooping shoots
- It was a simple step
- I was comfortable once a few bugs had been fixed with an upgrade

Q4. The CWSI results were what you expected

	Strongly Disagree	Disagree	Neutral	Agree	Strongly Agree
No. of people selected	1		3	10	2
Percentage of people selected	6.25 %	0 %	18.75 %	62.5 %	12.5 %

Comment summary:

- This season was not helpful for the water stress testing. Most vines didn't experience water stress. However in general results are good.
- As a general rule yes.
- Generally yes. Sometimes surprised to see stress when vines seemed OK.
- Noticed there was a significant difference between taking photos in early morning and later afternoon.
- The results matched the known dry patch and wet patch.
- In case of weak vines tended to pick up a region on a healthy vine in next row.

- Had no confidence in the result. The plant looks healthy, but the app shows it had water stress. Maybe because the vine had small canopy. (Only used the app once in early stage)
- Yes. 90% of the time the results were as predicted.
- The CWSI figures were as I thought when looking at the vines during different times of the day and knowing the soil moisture levels.
- It matched what we saw visually and on our soil moisture monitoring.
- We are a cool site and so it was what we expected

Q5. I considered the weather conditions when making measurements and interpreting results.

	Strongly Disagree	Disagree	Neutral	Agree	Strongly Agree
No. of people selected		1	3	6	6
Percentage of people selected	0 %	6.25 %	18.75 %	37.5 %	37.5 %

Comment summary:

- Restricted by time
- Used on hot days >32^{0}C
- Considered the sun direction and sun movement
- Tried in all weather conditions
- I tried to sample in the morning, mid-afternoon then late afternoon. Windy conditions were found to be hard to capture good images. Tried the app in hot conditions (39 degrees) and found the vines to be shut down, and this was to be expected.
- I paid attention to cloud cover, rainfall and vine stress level.

Q6. The CWSI figures were useful in making irrigation decisions

	Strongly Disagree	Disagree	Neutral	Agree	Strongly Agree
No. of people selected			6	8	2
Percentage of people selected	0 %	0 %	37.5 %	50 %	12.5 %

Comment summary:

- It is a useful tool. However due to the very wet season, did not even turn the water on. If we irrigated I would have used this tool as a reference.
- Season didn't help for app testing
- I think over time as I use the tool more often, then this will be the case. At this stage it is similar to soil moisture monitoring which I use as part of the decision.
- Did not use so much for irrigation rather to monitor stress of vines with root disease
- If had chance to use more times, I would have a better understanding of the CWSI, and it could be useful in making irrigation decisions.

- Yes. I cross referenced with soil moisture results and they were as expected.
- Quick & easy tool.
- The CWSI figures were more of a confirmation on the duration of irrigation applied and the timing of the applications were correct as you could determine the amount of stress you are applying.
- Our irrigation system runs 24hrs/day on continuous rotation. This region (Riverland) is hot and low rainfall, very limited options to change irrigation strategy.

Q7. Would you consider using the app in the future?

	Yes	No	Not Sure
No. of people selected	13	2	1
Percentage of people selected	81.25 %	12.5 %	6.25 %

Comment summary:

- Enjoyed using the app.
- Yes, but the app needs more development.
- The beauty of the app is you can measure the vines everywhere.
- Definitely
- Cheap, quick + easy. Good back up to soil moisture readings
- Yes, definitely I would consider using the app in the future as long as the process in collecting wet and dry temperatures within the vines were easier.
- Yes I can see a use for it to help in scheduling irrigation
- Not relevant as our system can't vary. Our block is big and the water is always on.
- The app itself was good to use but it was the paddles that made it a bother to use as it took up time.

Q8. Would you recommend the app to others?

	Yes	No	Not Sure
No. of people selected	14		2
Percentage of people selected	87.5 %	0 %	12.5 %

Comment summary:

- Will be interested to see how the development goes.
- Yes. Already have and will continue to
- The app is a great tool to determine and to confirm the user's observations and thoughts when determining whether to apply or hold off on irrigation.
- I think the app would be great for growers with smaller areas to manage, and systems that have flexibility.
- It can help young and inexperienced growers.
- Simple, easy to use, instantaneous results

- That’s a yes/no as if the procedure changed involving the paddles.

Q9. Do you have any suggestions for improving the app?

- Once it’s calibrated for the site/manager, if the result number could come up in a colour code (colored bar) to indicate the stress level, it could be helpful.
- If it works on iPhone, it will be great
- Need to consider the orientation of the row to determine taking images in the morning or in the afternoon.
- Need to modify the wet and dry references to make them easier and quicker to install on the vine.
- Automated system to enable seeing progression through the day rather than a ‘point in time’ sample. Data logger system?
- Fix both references into a frame. Easier to carry.
- Maybe multiple wet and dry references can be fixed in certain spots rather than carrying them around. For example install them on the vine near a G-Bug system or a weather station. People can download the data and take a picture at the same time. This could help this app be more acceptable to the industry.
- Suggest to create app that works without reference leaves.
- Would like the app to locate the block by GPS. Once you take a photo, the block name automatically pops up.
- The final version of the app should give users the opportunity to send the spreadsheet (.CSV?) with the results via email.
- The final version should also have clearer clues about how to move from one screen to the other, e.g. how to move back from the results screen to the initial screen.
- Too busy to have time to test it. Only used once during the season, weather during season not conducive to stress development, so limited feedback.
- Multiple cameras in different sites to provide logging could be considered.
- Need to have less error and lag when using the App.
- Making the references smaller in size and with smaller water bottle would help with carrying and installing.
- The app could send the image straight to the user’s computer with all of the information. Save time downloading the image from the phone.
- Could temperatures of wet and dry references be pre-loaded in to the app to remove the need for adding the references to the canopy every time?

Appendix 6: Budget reconciliation

The End of Project Financial Statement was submitted online via Wine Australia's Clarity Investment Management System.